

Published in final edited form as:

*Nat Med.* 2015 May ; 21(5): 467–475. doi:10.1038/nm.3842.

## Homeostatic regulation of T cell trafficking by a B cell derived peptide is impaired in autoimmune and chronic inflammatory disease

Myriam Chimen<sup>#1</sup>, Helen M. McGettrick<sup>#2</sup>, Bonita Apta<sup>1</sup>, Sahithi J. Kuravi<sup>1</sup>, Clara M. Yates<sup>1</sup>, Amy Kennedy<sup>1,10</sup>, Arjun Odedra<sup>1</sup>, Mohammed Alassiri<sup>1</sup>, Matthew Harrison<sup>1</sup>, Ashley Martin<sup>3</sup>, Francesca Barone<sup>2,5</sup>, Saba Nayar<sup>2</sup>, Jessica R. Hitchcock<sup>4</sup>, Adam F. Cunningham<sup>4</sup>, Karim Raza<sup>2,5</sup>, Andrew Filer<sup>2,6</sup>, David A. Copland<sup>7</sup>, Andrew D. Dick<sup>7,8</sup>, Joseph Robinson<sup>1</sup>, Neena Kalia<sup>1</sup>, Lucy S. K. Walker<sup>9</sup>, Christopher D. Buckley<sup>2,5</sup>, Gerard B. Nash<sup>1</sup>, Parth Narendran<sup>‡,1,10</sup>, and G. Ed. Rainger<sup>‡,\*,1</sup>

<sup>1</sup>School of Clinical and Experimental Medicine, University of Birmingham, Birmingham, UK

<sup>2</sup>Rheumatology Research Group, Arthritis Research UK Centre of Excellence in the Pathogenesis of Rheumatoid Arthritis, School of Immunity and Infection, College of Medical and Dental Sciences, University of Birmingham, Birmingham, UK

<sup>3</sup>School of Cancer Sciences, University of Birmingham, Birmingham, UK

<sup>4</sup>School of Immunity and Infection, University of Birmingham, Birmingham, UK

<sup>5</sup>Department of Rheumatology, Sandwell and West Birmingham Hospitals NHS Trust, Birmingham, UK

<sup>6</sup>Department of Rheumatology, University Hospitals Birmingham NHS Foundation Trust, Birmingham, UK

<sup>7</sup>Academic Unit of Ophthalmology, School of Clinical Sciences, University of Bristol, Bristol, UK

<sup>8</sup>National Institute for Health Research Biomedical Research Centre at Moorfields Eye Hospital NHS Foundation Trust and UCL Institute of Ophthalmology; University Hospitals Bristol NHS, Foundation Trust, and University of Bristol, UK

<sup>9</sup>Institute of Immunity & Transplantation, UCL Medical School, Royal Free Campus, London, UK

Users may view, print, copy, and download text and data-mine the content in such documents, for the purposes of academic research, subject always to the full Conditions of use:[http://www.nature.com/authors/editorial\\_policies/license.html#terms](http://www.nature.com/authors/editorial_policies/license.html#terms)

\*Correspondence to: Correspondence and request for material should be addressed to GER (G.E.Rainger@bham.ac.uk) and PN (p.narendran@bham.ac.uk).

**AUTHORS CONTRIBUTIONS** MC conceived and performed experiments, analyzed and interpreted the data, and co-wrote the manuscript. HMM conceived, performed experiments, analyzed and interpreted the data. BA, SJK, CMY, AK, AO, MA, MH, SN, JRH, DAC and JR performed experiments and analysed the data. AM, FB, AFC, KR, AF, DAC, ADD, NK, LSKW, CDB and GBN organized and conducted the study including analysis and interpretation of data and critique of the manuscript. KR and AF recruited and diagnosed patients in early arthritis clinics, and acquired the clinical data. PN conceived, designed and organized the T1D study as well as analyzing and interpreting the data. GER conceived, designed, organized and conducted the study, including analysis and interpretation of data and co-wrote the manuscript.

‡These authors contributed equally to the supervision of this work

**SUPPLEMENTAL INFORMATION** Supplemental information includes nine figures and eight tables -PDF.

**Competing financial interests:** The other authors have no competing financial interests to declare.

<sup>10</sup>Department of Diabetes, University Hospitals Birmingham NHS Foundation Trust, Birmingham, UK

# These authors contributed equally to this work.

## Abstract

During an inflammatory response, lymphocyte recruitment into tissue must be tightly controlled because dysregulated trafficking contributes to the pathogenesis of chronic disease. Here we show that during inflammation and in response to adiponectin, B cells tonically inhibit T cell trafficking by secreting a peptide (PEPITEM) proteolytically derived from 14.3.3.ζδ protein. PEPITEM binds cadherin-15 on endothelial cells, promoting synthesis and release of sphingosine-1 phosphate, which inhibits trafficking of T cells without affecting recruitment of other leukocytes. Expression of adiponectin receptors on B cells and adiponectin induced PEPITEM secretion wanes with age, implying immune senescence of the pathway. Additionally, these changes are evident in individuals with type-1-diabetes or rheumatoid arthritis, and circulating PEPITEM in patient serum is reduced compared to healthy age matched donors. In both diseases, tonic inhibition of T cell trafficking across inflamed endothelium is lost. Importantly, control of patient T cell trafficking is re-established by exogenous PEPITEM. Moreover, in animal models of peritonitis, hepatic I/R injury, Salmonella infection, Uveitis and Sjögren's Syndrome, PEPITEM could reduce T cell recruitment into inflamed tissues.

## INTRODUCTION

In vertebrates, a lymphocyte (T cell and B cell) based adaptive immune system has evolved to augment innate immunity. Adaptive responses require lymphocyte trafficking between the bone marrow, lymphoid organs and peripheral tissues using blood as a vehicle for dispersal<sup>1</sup>. Understanding of the trafficking process is still incomplete. However, unregulated T cell recruitment during inflammation is pathogenic and contributes to chronic disease<sup>2,3</sup>. Here we reveal the function of a homeostatic pathway, which imposes a tonic inhibition on T cell trafficking during inflammation. Identification of this pathway arose through studies on the circulating adipokine, adiponectin. Adiponectin affects both metabolic and immune pathways<sup>4-7</sup>, including the recruitment of leukocytes during an inflammatory response<sup>6</sup>, and plasma concentrations are low in a number of chronic diseases, including diabetes<sup>4</sup>. For the first time we tested the hypothesis that adiponectin might regulate lymphocyte trafficking and that changes in adiponectin function might contribute to pathogenic lymphocyte recruitment in chronic inflammatory and autoimmune diseases.

We started by observing lymphocyte trafficking *in vitro* across isolated human endothelial cells, which are the gatekeepers to the tissues for circulating leukocytes. To enter inflamed tissue, T cells migrate through endothelial cells lining the post-capillary venules<sup>8,9</sup>, and this has been modelled both *in vitro* and *in vivo*<sup>10-15</sup>. Thus, memory T cells moving rapidly in the flowing blood are preferentially recruited by endothelial cells activated by cytokines (e.g. TNF-α and/or IFN-γ). Tethering from flow and rolling adhesion are supported by E-selectin and VCAM-1<sup>16</sup>, while integrin mediated stable adhesion and migration are supported by sequential signals from chemokines and prostaglandin-D<sub>2</sub><sup>17-23</sup>. Here we show

that in the presence of adiponectin, B cells recruited to the endothelial cell surface during inflammation reduce the efficiency of memory T cell migration by imposing a tonic inhibition on this process. Thus, we believe that the adaptive immune system has evolved a robust strategy for regulating inappropriate or excessive activity, thereby limiting the possibility of establishing a chronic inflammatory response which might contribute to disease.

## RESULTS

### Adiponectin regulates T cell migration

*In vitro*, adiponectin dose-dependently inhibited the TNF- $\alpha$  and IFN- $\gamma$  induced trans-endothelial migration of human peripheral blood lymphocytes (PBL) with an EC50 of 2.6 nM (0.94  $\mu$ g/ml) (Fig. 1a, Supplementary Fig. 1a), with the most marked effects seen at physiological circulating levels observed in healthy humans (5–15  $\mu$ g/ml). Although migration was reduced so that more cells were firmly adherent to the apical surface of the endothelium (Supplementary Fig. 1b), the number of lymphocytes recruited was unaffected by adiponectin (Supplementary Fig. 1c). The effects of adiponectin on PBL migration were seen in both a static system (Fig. 1a), and under conditions of flow (Fig. 1b), and were evident on human umbilical vein endothelial cells (HUVEC), or human dermal microvascular endothelial cells (HDMEC) (Fig. 1c). The majority of transmigrating PBL were CD3<sup>+</sup>CD45RO<sup>+</sup>memory T cells, as expected for this model (<sup>17</sup> and data not shown). Adiponectin did not alter the expression and/or function of lymphocyte integrins ( $\alpha_4\beta_1$  and  $\alpha_L\beta_2$ ), the CXCR3 chemokine receptor, or the PGD<sub>2</sub> receptor (DP-2) on PBL (Supplementary Fig. 1d). Moreover, chemotactic responses to CXCL12, CXCL10, or PGD<sub>2</sub> were unaltered by adiponectin (Supplementary Fig. 1e). Less than 5% of T cells (CD3<sup>+</sup> cells), including memory and naïve subsets, expressed adiponectin receptors (AdipoR1 and AdipoR2) (Fig. 1d-f). However, circulating B cells (CD19<sup>+</sup> cells) expressed both receptors abundantly (Fig. 1d-f). We also found that endothelial cells expressed both adiponectin receptors (Supplementary Fig. 2). However, adiponectin did not directly target endothelial cells in our system, as treated PBL are washed to remove any adiponectin prior to their addition to the endothelial cells. To ensure that any residual carryover of this agent did not influence lymphocyte recruitment, we verified that adiponectin did not modulate the gene expression of adhesion molecules and chemokines in TNF- $\alpha$  and IFN- $\gamma$  stimulated endothelial cells (Supplementary Table 1). As T cells lack adiponectin receptors but show altered patterns of migration in response to adiponectin, we postulated that another lymphocyte population mediated the inhibition of T cell trafficking. Upon depleting B cells from the PBL mixture, T cells were released from the inhibitory effects of adiponectin (Fig. 1g). Adding back purified B cells to isolated T cells could reconstitute the adiponectin-dependent inhibition of T cell migration, and using supernatants from adiponectin stimulated B cells was as effective as addition of B cells themselves (Fig. 1g). The ability of B cell supernatants to impair T cell migration was lost when B cells were activated with adiponectin in the presence of an inhibitor of protein secretion, brefeldin-A (Fig. 1g). These experiments suggest B cells release a soluble factor in response to stimulation by adiponectin that regulates migration of T cells.

## Adiponectin induces PEPITEM secretion by B cells

We utilized an unbiased proteomic screen to identify the agent(s) secreted by purified B cells following stimulation with or without adiponectin. A comparative analysis identified a 14 amino-acid peptide, SVTEQGAELSNEER, specific to the supernatants of adiponectin stimulated B cells (Fig. 2a). Comparing this to an *in silico* library of published and predicted sequences, the peptide demonstrated 100% sequence homology to a single human protein, and represents amino acids 28–41 of the 14.3.3 zeta delta (14.3.3.ζδ) protein, which in turn is a 245 amino-acid product of the *YWHAZ* gene (Fig. 2b).

Proteolytic release of the peptide from the parent protein was confirmed after a tryptic digestion of recombinant 14.3.3.ζδ generated the same 14 amino-acid product (Supplementary Table 2). A time course of the 14.3.3.ζδ derived peptide secretion from adiponectin stimulated B cells showed rapid and sustained release (Supplementary Fig. 3a). A synthetic peptide exhibited an identical mass:charge (*m/z*) ratio to that of the native peptide (*m/z*=774.88), suggesting the B cell derived product was not subject to post-translational modification prior to secretion (Supplementary Fig. 3b, c). Synthetic peptide showed a dose-dependent inhibitory effect on the trafficking of PBL across TNF-α and IFN-γ stimulated endothelial cells *in vitro* (Fig. 2c), with an EC<sub>50</sub> of 19 pM (28 pg/ml) (Supplementary Fig. 4a). A similar response was observed in the absence of bovine serum albumin, which removed any source of arachidonic acid that might be used to generate bioactive eicosanoids such as PGD<sub>2</sub>, which are known to regulate T cell trafficking<sup>23</sup> (Supplementary Fig. 4b). Like adiponectin, the peptide had no effect on the number of lymphocytes adherent to the endothelial cells (Supplementary Fig. 4c), but it increased the number of surface adherent cells, as migration through the monolayer was inhibited (Supplementary Fig. 4d). A scrambled peptide, containing the same amino acids in random order, or other peptides of unrelated sequence but with known biological activity (proinsulin chain A peptide and tetanus toxoid peptide), had no effect on T cell migration (Fig. 2c). As the peptide inhibited T cell migration we named it **PEP**ptide **I**nhibitor of **T**rans-**E**ndothelial **M**igration; PEPITEM. PEPITEM specifically inhibited the migration of CD4<sup>+</sup> and CD8<sup>+</sup> memory T cells, without affecting transmigration of neutrophils or monocytes (Fig. 2d), nor the total adhesion of any leukocyte subset (Supplementary Table 3 and 4 for adiponectin). In addition, PEPITEM inhibited T cell transmigration on both HDMEC and HUVEC (Supplementary Fig. 4e). PEPITEM was ineffective if PBL were pre-treated, and only had inhibitory effects when pre-incubated on endothelial cells, implying that PEPITEM operated by stimulating a receptor on these cells (Supplementary Fig. 4f). When we fractionated B cells into their subsets, we found that plasma cells (CD38<sup>+++</sup>IgD<sup>-</sup>IgM<sup>-</sup>CD27<sup>-</sup>) were able to secrete higher quantities of PEPITEM compared to naïve (CD38<sup>+</sup>IgD<sup>+</sup>IgM<sup>+</sup>) or memory (CD38<sup>-</sup>IgD<sup>-</sup>IgM<sup>-</sup>CD27<sup>-</sup>) B cells following incubation with adiponectin (Supplementary Table 5). There was also an enrichment of plasma cells on cytokine stimulated endothelial cells (Supplementary Fig. 4g). These data imply a dominant role for circulating plasma cells in the regulation of memory T cell trafficking.

## The endothelial cell receptor for PEPITEM is Cadherin-15

To identify a PEPITEM receptor on endothelial cells, we utilized PEPITEM with a biotin conjugate on the N-terminus as ‘bait’ to ‘fish’ for binding partners on the endothelial cell

surface. This peptide showed full efficacy in a functional migration assay (Supplementary Fig. 5a). PEPITEM-bound molecules were co-immobilized on neutravidin columns after endothelial cell lysis. Proteins eluted from the neutravidin columns were subject to analysis by mass-spectrometry for identification. This strategy yielded a candidate with a strong statistical score ( $>30$ ), cadherin-15 (CDH15; M-cadherin). CDH15 was efficiently knocked down in endothelial cells by specific siRNA oligomers, but not by control sequences (Fig. 2e, g and Supplementary Fig. 5b). Silencing of CDH15 did not alter the baseline efficiency of T cell migration across the endothelium (Supplementary Fig. 5c). However, it did release T cells from the inhibitory effects of PEPITEM (Fig. 2f). Binding data indicates that PEPITEM is able to bind recombinant CDH15 in a Biacore assay ( $KD=108.9 \mu M$ ) (Supplementary Fig. 5d).

CDH15 has not previously been described in endothelial cells, and here we show that mRNA for *CDH15* is endogenously expressed, as well as being up-regulated when endothelial cells are stimulated with inflammatory cytokines (Fig. 2e). In addition, CDH15 expression and up-regulation by cytokines in HDMEC was detected at a protein level using western blotting (Fig. 2g). Confocal microscopy also showed expression in HDMEC and skeletal muscle cells (SkMC, used as a positive control) using fluorescently labelled reagents, and staining was reduced following siRNA-mediated silencing of *CDH15*, demonstrating the specificity of the antibody (Fig. 2g, h and Supplementary Fig. 5b).

### Endothelial cell Sphingosine-1-phosphate impairs migration

Sphingosine-1-phosphate (S1P) is a biologically active sphingolipid generated in the cytosol from sphingosine, which is phosphorylated by the sphingosine kinases (SPHK), SPKH1 or SPHK2<sup>19</sup>. The endothelial cell transporter, spinster homolog 2 (SPNS2), is also necessary for translocation of S1P into extra-cellular fluid<sup>24-26</sup>. S1P plays an important regulatory role in the movement of T cells from inflamed tissue to afferent lymphatics<sup>27</sup> and for T cell egress from secondary lymphoid organs<sup>28-31</sup>. Here we found the S1P receptor antagonist, W146 (trifluoroacetate salt), released T cells from the inhibitory effects of both adiponectin and PEPITEM (Fig. 3a, b). Moreover, the effects of adiponectin and PEPITEM on T cell migration could be mimicked dose-dependently, when exogenous S1P was added to purified T cells (Fig. 3c). We confirmed that S1P was of endothelial origin by pre-treating endothelial cells with the SPHK1 inhibitor (2,2-dimethyl-4S-(1-oxo-2-hexadecyn-1-yl)-1,1-dimethylester-3-oxazolidinecarboxylic acid) or the SPHK1/2 inhibitor (N,N-Dimethylsphingosine) which abolished the ability of PEPITEM to inhibit T cell migration (Fig. 3d, e). In agreement with the patterns of activity of these inhibitors, we found that SPHK1, but not SPHK2, was highly expressed in endothelial cells but not in B cells (Supplementary Fig. 6a), and that mRNA for *SPHK1*, but not *SPHK2*, was increased upon stimulation of endothelial cells with TNF- $\alpha$  and IFN- $\gamma$  (Fig. 3f). Knock-down of endothelial *SPNS2* mRNA also released T cells from the inhibitory effects of PEPITEM (Fig. 3g and Supplementary Fig. 6b-d). Addition of S1P to endothelial cells at a concentration equivalent to the total circulating concentration in plasma ( $\approx 0.2 \mu M$ )<sup>32</sup> inhibited T cell transmigration efficiently (Fig. 3c). However, in the circulation S1P is bound to plasma proteins such as albumin and lipoproteins<sup>32, 33</sup> which limit its availability. Published data estimates that biologically active S1P circulates at approximately 5 nM<sup>33, 34</sup>. In the presence of this

concentration of S1P, the effects of PEPITEM on migration were readily observable (Supplementary Fig. 6e-g). Moreover, PEPITEM inhibition of T cell trafficking in the presence of 5 nM S1P could be reversed by treating endothelial cells with SPHK inhibitors or by *SPNS2* knock-down in these cells, showing that additional and functional S1P was released in response to PEPITEM stimulation (Supplementary Fig. 6e-g).

The process of T cell egress from lymph nodes into blood results in rapid S1P-mediated internalisation of S1P-receptors (S1PR1 and S1PR4) from the surface of circulating T cells<sup>30, 31</sup>. Thus for S1P to be an effective mediator during T cell migration across endothelial cells, S1P-receptors on T cells require up-regulation. We observed a robust increase in the expression of S1PR1 on the cell surface of memory T cells that had been recruited by cytokine stimulated endothelial cells (Fig. 3h). Moreover, rapid up-regulation of surface S1PR1 was observed when memory T cells adherent to immobilized, recombinant ICAM-1, were stimulated by CXCL10 (Fig. 3i, Supplementary Fig. 7a). This mode of T cell activation could override the desensitisation pathways for S1PR1, as high expression was maintained even in the presence of 10  $\mu$ M of exogenous S1P (Supplementary Fig. 7a). Moreover, this was not due to the recruitment of a subset of cells with high S1PR1 expression, as these were not evident in the isolated T cells prior to addition to the ICAM-1 (Supplementary Fig. 7a). Thus, during the process of recruitment, chemokines presented by endothelial cells rapidly and sustainably induce expression of S1PR1 on memory T cells.

S1P down-regulates the affinity of the T cell integrin adhesion receptor  $\alpha_L\beta_2$  (LFA-1), reducing binding to ICAM-1 after stimulation with the chemokine CXCL10 (Fig. 3j, Supplementary Fig. 7b). This change in integrin function did not alter the levels of T cell recruitment, which is E-selectin and VLA-4 dependent, in this model of *in vitro* transmigration<sup>17</sup> and data not shown). However, in the presence of adiponectin (and therefore S1P) there was a modest increase in the number of cells rolling on the endothelial cell surface (Supplementary Fig. 7c). Taken together these data imply that S1P-mediated changes in the function of LFA-1 are able to interrupt the process of LFA-1 mediated trans-endothelial migration.

### PEPITEM is functional *in vivo*

As PEPITEM is derived from B cells, we conducted a series of studies in the BALB/c B cell-deficient mouse<sup>35</sup>. In a model of zymosan-induced peritonitis, more T cells trafficked into the peritoneal cavity in B cell-deficient mice (Fig. 4a). Injection of PEPITEM during challenge with zymosan inhibited trafficking of T cells into the peritoneum (Fig. 4a). Additionally, we tested the efficacy of PEPITEM in a model of systemic bacteraemia upon *Salmonella* Typhimurium infection in the C57BL/6 B cell-deficient mouse. *Salmonella* colonizes the spleen and liver during primary infection<sup>36</sup> where it promotes an inflammatory infiltrate into infectious foci. PEPITEM reduces the number of T cells resident in these infectious foci in *Salmonella* infected B cell-deficient animals (Fig. 4b), with a trend towards reduced T cells in PEPITEM-treated wild-type (WT) animals (Supplementary Fig. 8a, b). PEPITEM also abolished T cell recruitment in the hepatic sinusoids, with a concomitant increase in the number of free flowing T cells, after acute liver ischaemia and reperfusion injury in C57BL/6 WT mice, when assessed by realtime intravital microscopy

(Fig. 4c, d and Supplementary Fig. 8c). This observation is consistent with integrin mediated processes that support leukocyte tethering in the low shear environment of the hepatic sinusoids<sup>37, 38</sup>.

In a model of endotoxin-induced (LPS) autoimmune uveitis (ocular inflammation) in C57BL/6 WT mice, administration of PEPITEM with LPS into the eye reduced the number of T cells in the ocular infiltrate (Fig. 4e). PEPITEM also reduced T cell trafficking into the salivary glands of C57BL/6 WT mice challenged with a virally induced model of tertiary lymphoid organ formation, which mimics changes observed in the autoimmune rheumatic disease, Sjögren's syndrome<sup>39</sup> (Fig. 4f, g). In both uveitis and Sjögren's syndrome models, as well as in the zymosan-induced peritonitis (data not shown), B cells were recruited to the sites of inflammation and the number of B cells recruited was not affected by PEPITEM (Supplementary Fig. 8d, e). In addition, in the *in vivo* model of acute, resolving inflammation (peritonitis), the recruitment patterns of F4/80 macrophages and CD11c<sup>+</sup> cells were not affected at the time point used to assess T cell trafficking (Supplementary Fig. 8f, g).

### The PEPITEM pathway is impaired in disease and the elderly

Efficacy in *in vivo* models of inflammation prompted us to investigate whether the PEPITEM pathway was compromised in individuals with the T cell driven autoimmune disease, type-1-diabetes (T1D) or individuals with rheumatoid arthritis. Firstly, we measured the expression of AdipoR1 and AdipoR2 on the circulating B cells of individuals with T1D or rheumatoid arthritis, comparing these to healthy age and gender matched control donors. (Cohort statistics in Supplementary Table 6, 7 and 8). The expression of both AdipoR1 and AdipoR2 was reduced on B cells from individuals with T1D (Fig. 5a for % positive B cells and Supplementary Fig. 9a for representative intensity histograms) and with rheumatoid arthritis (Fig. 5b for % positive B cells and Supplementary Fig. 9a for representative intensity histograms) compared to healthy controls. We observed no difference in the expression of CD19 on B cells and in B cell number between healthy controls and individuals with T1D or rheumatoid arthritis, suggesting these differences reflect changes in AdipoR1 and AdipoR2 expression (Supplementary Fig. 9b, c). There was a positive correlation between the expression of AdipoR1 and AdipoR2 on B cells with the quantity of PEPITEM released by B cells upon stimulation with adiponectin (Fig. 5c, d). This was the case for both individuals with T1D and healthy controls (AdipoR2 only), although in individuals with T1D only low levels of PEPITEM could be detected, which reflected the paucity of expression of adiponectin receptors. In addition, we were able to detect low concentrations of PEPITEM in serum from healthy controls and this was reduced in individuals with T1D (Fig. 5e).

Decreased PEPITEM secretion by B cells released T cells from the inhibitory effects of adiponectin, so that there was no longer an inhibition of T cell migration in individuals with T1D (Fig. 5f) or those with rheumatoid arthritis (Fig. 5g). The effects of adiponectin could be mimicked by the addition of exogenous PEPITEM in the *ex vivo* migration assay, using lymphocytes from individuals with T1D or rheumatoid arthritis (Fig. 5f, g), meaning that

loss of tonic inhibition of T cell migration in these individuals could be readily replaced with appropriate PEPITEM treatment.

One of the major risk factors for developing chronic inflammatory or autoimmune diseases is age. Thus, we analyzed the expression of AdipoR1 and AdipoR2 in healthy donors of different ages. There was a negative correlation between the expression of AdipoR1 and AdipoR2 and age (Fig. 5h, i).

## DISCUSSION

The processing of an immune regulatory, 14 amino-acid peptide, from an intracellular protein (14.3.3 $\zeta\delta$ ) with no known association to the inflammatory response has not been described in, nor could it have been predicted from, any of the known pathways that regulate leukocyte trafficking. In fact, the functions of the 7 family members of the 14.3.3 protein family are diverse. For example, they are involved in regulating the function of cytosolic proteins which support metabolic, cell cycle, apoptotic and protein trafficking pathways<sup>40–42</sup>. Their importance in such homeostatic pathways is highlighted by their association with diseases as varied as cancer, hyper-proliferative skin disorders and Alzheimer's disease, when their function is disrupted<sup>43, 44</sup>. The effects of losing the function of the PEPITEM pathway that we document here now allows us to add T1D and rheumatoid arthritis to the list of diseases in which the dysregulated function of 14.3.3 proteins plays a role.

Here we showed that extracellular PEPITEM impaired lymphocyte trafficking by indirectly regulating the function of the  $\beta_2$ -integrin, LFA-1. Interestingly, both intracellular 14.3.3 $\beta$  and 14.3.3 $\zeta\delta$  have been implicated in the regulation of adhesion dependent cellular functions in other contexts. For example, morphology and adhesion in dendrites, embryonic kidney cell lines and rat fibroblasts, are associated with the 14.3.3 $\beta$  dependent regulation of  $\beta_1$ -integrins<sup>45–50</sup>. Moreover, 14.3.3 $\zeta\delta$  protein in platelets regulates the function of the adhesion complex GPIb/IX/V, and is required for efficient recruitment of platelets to von Willbrand factor (VWF)<sup>51</sup>. It is also notable that SIP, the terminal mediator in the PEPITEM pathway, can also regulate the function of endothelial cell borne adhesion receptors<sup>52, 53</sup> (e.g. VE-cadherin) which are involved in the regulated trafficking of leukocytes. Thus, although a role in lymphocyte trafficking is novel for 14.3.3 proteins; the regulation of adhesion molecules in other cells and contexts does provide a generic link between their known biological functions and the new role described here.

In the lymph node, a process of reciprocal crosstalk between B cells and T cells is known to be important in establishing an antigen specific immune response<sup>54</sup>. Crosstalk between B cells and T cells also plays a role in the initiation of T cell mediated autoimmune events in T1D and rheumatoid arthritis<sup>55, 56</sup>. Indeed, 'depletion' of B cells by the monoclonal antibody rituximab has beneficial effects in these diseases<sup>57, 58</sup>. It might be assumed that such a B cell depletion strategy might compromise the inhibitory effects of PEPITEM on T cell trafficking by removing the tonic 'brake' on inflammation provided by this pathway described in detail in Figure 6. However, our data implies that this pathway is no longer functional in individuals with established disease. Thus, it is unlikely that the benefit of



removing pathogenic B cells is being achieved at the expense of the protective functions of PEPITEM secreting B cells. However, our observation that exogenous peptide can regain control of the trafficking of patient T cells raises the possibility that the PEPITEM pathway may present a tractable target for the development of novel therapeutic agents with which to treat chronic inflammatory and autoimmune diseases. In T1D or rheumatoid arthritis this might be achieved using the peptide itself. However, we predict that in other disease states alternative aspects of this pathway may be compromised. For example, expression and proteolytic processing of 14.3.3.ζδ to yield mature peptide could be altered, as could the secretory pathways required for PEPITEM release in response to adiponectin. In endothelial cells, changes in the expression of cadherin-15, or the release of SIP in response to PEPITEM signalling could lead to inappropriate T cell trafficking. Lastly, T cells themselves may lose the capacity to respond to SIP by failing to upregulate S1PRs in response to inflammatory chemokines, or through alterations in the intrinsic signalling pathways lying downstream of these molecules. Many of these processes have yet to be defined mechanistically, for example, the identity and localisation of the protease(s) which cleave PEPITEM from 14.3.3. ζδ. However, with a fuller understanding of the biology of the PEPITEM pathway it will be important to determine whether alterations in these other steps are detectable in disease. If they are, they will represent unique opportunities to develop new therapeutic agents.

## ONLINE METHODS

### General

Alta Bioscience (University of Birmingham, Birmingham, UK) synthesized PEPITEM, scrambled peptide and biotinylated PEPITEM. We purchased Sphingosine-1-phosphate, W146 (trifluoroacetate salt), PGD2, SPHK1 inhibitor, 2,2-dimethyl-4S-(1-oxo-2-hexadecyn-1-yl)-1,1-dimethylester-3-oxazolidinecarboxylic acid, SPHK1 inhibitor 5c, and the SPK1/2 inhibitor, N,N-dimethylsphingosine from Cayman Chemicals (Michigan, USA). We purchased Chemokines and cytokines from Peprtech (London, UK) and R&D systems (Oxford, UK).

### Isolation of leukocytes

We obtained blood samples from healthy donors with written informed consent and approval from the University of Birmingham Local Ethical Review Committee (ERN\_07-058).

We isolated Peripheral blood mononuclear cells (PBMC) and neutrophils from blood using a two-step density gradient of Histopaque 1077 and 1119 (Sigma-Aldrich, Poole, UK). Lymphocytes were purified by panning PBMC on culture plastic for 30 minutes at 37°C to remove monocytes as previously described<sup>59</sup>. Peripheral Blood Lymphocytes (PBL) were then counted, resuspended in M199 (Life Technologies Invitrogen Compounds, Paisley, U.K.) containing 0.15% bovine serum albumin (BSA; Sigma-Aldrich) at  $1 \times 10^6$  cells/ml for transmigration assays, or in PBS containing 0.5% BSA and 2 mM EDTA (Sigma-Aldrich) for cell sorting. B cells were depleted from PBL by positive selection using anti-CD19 beads (Miltenyi Biotec, Surrey, UK). When B cells were reconstituted into PBL or used to

generate supernatants, B cells were sorted by negative selection in order to yield untouched cells (Stemcell, Grenoble, France). Memory and naïve CD4 and CD8 T cells were isolated using negative selection kits (StemCell). Monocytes and their subsets were isolated by positive selection using CD14 and CD16 beads (Miltenyi Biotec).

### ***In vitro* transmigration assay**

Human umbilical cords were obtained from the Human Biomaterials Resource Centre (HBRC, University of Birmingham) (09/H1010/75) which holds ethical approval and collected fully consented tissue from the Birmingham Women's Hospital NHS Trust. Human Umbilical Vein Endothelial cells (HUVEC) were isolated from umbilical cords as previously described<sup>60</sup> and cultured in M199 supplemented with 20% FCS (Foetal Calf Serum), 10 ng/ml epidermal growth factor, 35 µg/ml gentamycin, 1 µg/ml hydrocortisone (all from Sigma-Aldrich), and 2.5 µg/ml amphotericin B (Life Technologies Invitrogen Compounds). Primary HUVEC were dissociated using trypsin/EDTA (Sigma-Aldrich) and seeded on twelve-well tissue culture plates (Falcon; Becton Dickinson Labware), or iBidi chamber slides (iBidi, Martinsried, Germany) for adhesion assays in low serum medium 2% (Endothelial Basal Medium, Promocell, Heidelberg, Germany). Seeding density was chosen to yield confluent monolayers within 24 hours. TNF-α (100 U/ml; Sigma-Aldrich) and IFN-γ (10 ng/ml; PeproTech, London, U.K.) were added to confluent monolayers for 24 hours before adhesion assay with lymphocytes. Primary human dermal endothelial cells (HDMEC) were purchased from Promocell and cultured in the manufacturer's recommended medium (Endothelial cell growth medium) (Promocell,). HDMEC were used after four passages.

Prior to adhesion assay,  $1 \times 10^6$  PBL or  $1 \times 10^5$  B cells were treated with adiponectin (0.0001 to 15 µg/ml) at room temperature under agitation for one hour and washed prior to use. Static or flow based adhesion assays were performed as previously described<sup>18</sup>. EC were washed twice with M199 0.15% BSA to remove the excess cytokines. PBL were allowed to adhere to the EC for 6 minutes at 37°C before non-adherent cells were removed by washing with M199 0.15% BSA. PBL adhesion and migration was assessed using a phase-contrast videomicroscope as previously described<sup>61</sup>. Manipulations and microscopy were carried out at 37°C. Recordings were digitized and analyzed offline using Image-Pro Plus software (DataCell, Finchampstead, U.K.). The numbers of adherent cells were counted in each field, averaged and converted to cells per mm<sup>2</sup> and multiplied by the known surface area of the EC monolayer to calculate the total number adherent. This number was divided by the known total number of PBL added to obtain the percentage of the PBL that had adhered. Each lymphocyte was classified as either: 1) phase bright and adherent to the surface of the EC; or 2) phase dark and spread and migrating below the EC. The percentage of adherent lymphocytes that had transmigrated was calculated. In some experiments, data was normalized to the control by dividing the percentage transmigration of the treated sample by the percentage of transmigration of the control and multiplied by 100.

For the B cell reconstitution experiments, B cells were negatively selected using StemSep magnetic kit and 100,000 cells incubated with 15 µg/ml adiponectin for one hour at room temperature. Cells were centrifuged 1500 rpm for 7 minutes and 1 ml of supernatant was added to  $1 \times 10^6$  B cell-depleted PBL (1 B cell to 10 B cell-depleted PBL). Negatively sorted

B cells (100,000) were incubated with Brefeldin-A (10 µg/ml) for 4 hours and adiponectin (15 µg/ml) for the last hour. Cells were then washed and supernatant added back to B cell depleted PBL and transmigration was measured.

In some experiments, lymphocytes were pre-treated with 10 µM S1PR antagonist (W146) or S1P (0.0001 to 100 µM) at room temperature under agitation and washed after 30 minutes, so the treatments did not modulate HUVEC function. Alternatively, HUVEC or HDMEC were pre-treated with 5 µM of SPHK1 or SPHK1/2 antagonists at 37°C and washed after 30 minutes. PEPITEM was added to the PBL or different leukocyte subsets at room temperature under agitation and washed after 30 minutes, so the treatments did not modulate HUVEC function, prior incubation of cells on EC.

Firmly adhered PBL were collected from the EC surface using cold EDTA for 3 washes. Transmigrated PBL were collected by treatment of EC with accutase (Sigma-Aldrich). Both fractions were labelled and analyzed by flow cytometry as described below in the **Flow cytometry** section.

### Flow cytometry

PBMC were stained with the relevant antibodies for 30 minutes at 4°C. Subsequently, samples were labelled with the relevant secondary conjugated antibodies for 30 minutes at 4°C. Isotype controls and secondary only conditions were used as negative controls. Rabbit anti-human AdipoR1 (357–375) and AdipoR2 (374–386) antibodies (Phoenix pharmaceuticals, Karlsruhe, Germany) were used at 5 µg/ml, and detected using a goat-anti rabbit Alexa 488 secondary antibody used at 8 µg/ml (Life Technologies Invitrogen Compounds). Gating to measure the expression of AdipoR1 and AdipoR2 on PBL and B cells was based on the isotype control. Isotype control frequencies were subtracted from the AdipoR1 and AdipoR2 frequencies for each subject. The following antibodies were used to stain human PBMC: CD4-FITC (1:50) (OKT-4), CD3-PerCp-Cy5.5 (1:50) (OKT3), CD19-PECy7 (1:50) (HIB19), CD8-Pacific Blue (1:50) (OKT8), CD56-PE (1:50) (MEM188) (all from E-bioscience, Hatfield, UK), CD4-Pacific orange (1:10) (clone S3.5) (Life Technologies Invitrogen Compounds) and CD45RO-APC (1:20) (UCHL1) (BD Bioscience, Oxford, UK),  $\alpha_4\beta_1$ -PE (1:100) (P5D2),  $\alpha_1\beta_2$ -FITC (1:100) (212701), DP-2-FITC (1:10) (301108) (R&D Systems, UK.), CXCR3-PE (1:50) (2Ar1) (US Biological). B cell subsets were labelled using CD19-PerCp-Vio700 (1:30) (LT19), IgM-PE (1:30) (PJ2-22H3), IgD-APC (1:60) (IgD26), CD38-FITC (1:150) (IB6) and CD27-APC-Vio-770 (1:10) (M-T271) (all from Miltenyi Biotec).

The following antibodies were used to stain mouse PBMC from blood and peritoneal lavage: CD3-FITC (1:50) (145-2C11), CD3-PECy7 (1:50) (145-2C11), CD4-PB (1:100) (GK1.5), CD8-TR (1:200) (5H10), CD11C-PECy7 (1:50) (N418), CD19-APC (1:50) (1D3), CD44-FITC (1:500) (IM7), CD45-PerCpCy5.5 (1:200) (30-F11), CD62L-PE (1:500) (MEL-14), B220-APCCy7 (1:100) (RA3-6B2), gp38-PE (1:200) (8.1.1) (all from Ebioscience) and F4/80-APC (1:20) (CI:A3-1) (AbD Serotec, Kidlington, UK). Samples were assayed using a Cyan (Dako) with Summit software and then analyzed using FlowJo software (Tree Star, Ashland, OR). Between 10,000 and 50,000 events per sample were recorded and plotted as frequency of positive cells or mean fluorescence intensity (MFI).

## Confocal Microscopy

Cells were grown to confluence onto glass chamber slides (Becton Dickinson Falcon) at 37°C. They were then fixed with 2% formaldehyde and 4% sucrose for 15 minutes, washed in PBS and stained with 10 µg/ml of either a sheep anti-human CDH15 antibody (Val22-Ala606) (R&D systems) or sheep IgG (Southern Biotech, UK) overnight at 4 °C. Goat anti-sheep IgG1 conjugated to Alexa 488 (1:1000) (Abcam, UK) was then applied and the slides were visualized using a Zeiss LSM 510 inverted laser scanning confocal microscope using a X40 water immersion objective with excitation at 488 nm and 543 nm (Zeiss, Gottingen, Germany). Constant acquisition parameters and laser power were maintained throughout individual experiments for analysis and images were processed using Zeiss LSM Image Examiner software (Zeiss). Digital images were recorded in two separately scanned channels with no overlap in detection of emissions from the respective fluorochromes. Confocal micrographs were stored as digital arrays of 1024×1024 pixels with 8-bit sensitivity.

## Immunoprecipitation and Western Blotting

Whole cell lysates were extracted by suspending cells in lysis buffer with 50 mM Tris-HCl pH 8, 150 mM NaCl, 10% glycerol, 1% (w/v) Nonidet P-40, 0.5% (w/v) sodium deoxycholate, and protease inhibitor cocktail (Invitrogen). After incubation for 15 minutes at 4 °C, this preparation was centrifuged at 600 g for 10 minutes. The supernatant was subjected to immunoprecipitation by incubating for 30 minutes at 4°C with protein G-Dyna beads (Invitrogen) and polyclonal sheep anti-CDH15 antibody (10 µg/ml) (Val22-Ala606) (R&D systems). The beads were collected and washed three times with ice-cold extraction buffer and once with 50 mM Tris-HCl pH 7.5. Proteins that were retained on the beads were eluted using 50 mM Glycine pH 2.8 and separated by SDS-PAGE 10% (w/v) and analyzed by western blot with a sheep anti-human CDH15 antibody (1 µg/ml) (Val22-Ala606) (R&D systems). Blots were then probed with appropriate horseradish peroxidase-conjugated anti-sheep secondary antibody (1:3000) (Cell Signalling Technology, UK). Immunodetection was carried out using the ECL plus Kit (Amersham, GE Healthcare Life Sciences, and UK) followed by exposure to X-ray film for 15 minutes. Controls were run in parallel with application of the recombinant CDH15 (R&D systems).

## siRNA transfection

HUVEC were plated in 12 well plates (87,500 cells per well) for 24 hours or until about 80% confluence. The relevant siRNA were added at a final concentration of 50 nM to 83.75 µl or 82.5 µl if duplex in Optimem media (Life Technologies Invitrogen Compounds). 1.5 µl of RNAi Lipofectamine (Life Technologies Invitrogen Compounds) was mixed with 13.5 µl of Optimem and incubated for 10 minutes at room temperature. 15 µl of Lipofectamine mix was added to each siRNA singleplex or duplex, gently mixed, and incubated for a further 10 minutes. HUVEC were washed twice with PBS and 400 µl of Optimem was added to the Lipofectamine siRNA duplexes. After gentle agitation, the mix was added to the HUVEC and incubated at 37°C for 4 hours. The mix was then replaced with low serum media without antibiotics. After 48 hours, HUVEC were stimulated with TNF-α and IFN-γ for 24 hours before measuring PBL adhesion and migration as described previously. The

PEPITEM receptor candidate was targeted by four siRNA oligomers that were purchased from Qiagen (Crawley, UK); CHD15 (#1: ATCGCCGACTTCATCAATGAT, #2: CACAGCCCTCATCTATGACTA, #3: CCCGATCAGCGTATCCGAGAA, #4: CAGGACGACCTTCGAGACAAT) and the S1P transporter SPNS2 (#1: CTGCACTTCTGCTGCAATCAA, #2: CCCACACAACCTTGCTGGGCAA, #3: CAGCTTGGGCAACGTGCTCAA, #4: TGCCATTGGGACAATGAAGAA). Control random siRNA were purchased from ThermoScientific.

### Real-time PCR

Total mRNA was extracted using the RNeasy Minikit (Qiagen, Crawley, UK) according to the manufacturer's protocol. Briefly, PBMC were first lysed, then added to a column, after three washes, mRNA was eluted from the column with water. mRNA concentration was measured using Nanodrop spectrofluorimeter (LabTech) and mRNA was stored at  $-80^{\circ}\text{C}$ . To convert mRNA to cDNA, random primers (Promega, Maddison, USA) were annealed to 1  $\mu\text{g}$  of mRNA for 5 minutes at  $70^{\circ}\text{C}$ , after which the following mastermix was added to give a final volume of 30  $\mu\text{l}$ : 10 U Superscript II Reverse Transcriptase (RT), 10 U RNAout RNase inhibitor, 1X Superscript Buffer (all from Invitrogen) and 10 mM dNTPs (Promega). The reaction was run at  $37^{\circ}\text{C}$  for 1 hour, followed by 5 minutes at  $95^{\circ}\text{C}$ . To analyze mRNA, FAM-labelled SPHK1, SPHK2 and SPNS2 primers and VIC-labelled 18S primers were bought as Assay on Demand kits from Applied Biosystems (Warrington, U.K.). Samples were amplified in duplicates using the 7500HT Real-Time PCR machine (Applied Biosystems) and analyzed using the software package SDS 2.2 (Applied Biosystems). Data were expressed as relative expression units relative to 18S or as fold change ( $2^{-\Delta\Delta\text{Ct}}$  method).

### Identification of PEPITEM

B cells ( $2 \times 10^5$ – $5 \times 10^5$ ) were incubated in presence or absence of adiponectin at 15  $\mu\text{g}/\text{ml}$ . Adiponectin (15  $\mu\text{g}/\text{ml}$ ) was added in M199 and used as a negative control. The peptides from the three samples were purified using C18 solid phase extraction columns from Supelco (DSC-18, Sigma-Aldrich). The columns were conditioned by adding 1ml of 0.1% trifluoroacetic acid (TFA, ThermoScientific) in acetonitrile (ACN, ThermoScientific), which like all additions was allowed to drip through the column under gravity. The column was then equilibrated with 0.1% TFA/water and the sample, adjusted to 0.1% TFA, was added to the column. The column was washed with 1 ml of 0.1% TFA/water and the peptides eluted using 0.1% TFA/acetonitrile (1ml) which was dried under vacuum and the samples resuspended in 20  $\mu\text{l}$  in 0.1% formic acid in 2% acetonitrile. 10  $\mu\text{l}$  of the purified samples was subjected to a LC-MS/MS analysis using a gradient of 2–36% ACN in 0.1% formic acid over 30 minutes at 350 nL/min using a Dionex Ultimate 3000 HPLC system. The HPLC column was connected to a Bruker ETD Amazon ion trap mass spectrometer with an online nanospray source. An MS survey scan from 350 to 1600 m/z was performed and the five most intense ions in each survey scan were selected for CID (collision induced dissociation) fragmentation. After ions were fragmented twice they were placed on an exclusion list for 0.5 minute. The raw data was processed using the Bruker DataAnalysis peak detection program to select peaks which were then searched using the Mascot search engine (version 2.1) using the SwissProt protein database. The minimum mass accuracy for both the MS and

MS/MS scans were set to 0.5 Da and no protease selection was used. The peptides were filtered using a minimum Mascot score of 30. The data output was analyzed via the Bruker ProteinScape software package. To identify a potential candidate in the B cell supernatant with adiponectin treatment, we applied a subtractive data analysis method. Hits from the adiponectin stimulated sample were compared to the B cell supernatant without adiponectin and recombinant adiponectin controls and common analytes were discarded. The recombinant 14.3.3.ζδ protein (100 µg) (Fitzgerald industries international, Acton, US) was digested using trypsin at 40 µg/ml (in 10% ACN, 90% HPLC dH<sub>2</sub>O, 0.1% TFA) for one hour at 37°C and samples were purified on C18 columns with at 90% ACN and analyzed using MS and database search as previously described above.

### Identification of PEPITEM receptor

EC were incubated with an N-terminus biotinylated version of PEPITEM or biotinylated scrambled control for four hours at 4°C. Cells were then wash twice in cold PBS and lysed with a Triton phosphate buffer (20 mM Sodium phosphate pH 7.5, 150 mM NaCl, 1% Triton X100, Protease inhibitor, all from Sigma-Aldrich). After 30 minutes, lysates were collected and centrifuged 20 minutes at 600 g at 4°C. Supernatants were collected and dried under vacuum and the samples resuspended in 20 µl 8 M Urea/2% SDS and loading buffer (Sigma-Aldrich and Life Technologies Invitrogen Compounds). Samples were loaded onto a 4–12% SDS-PAGE gel (Life Technologies Invitrogen Compounds) and stained overnight with Colloidal Coomassie staining buffer (0.08% Coomassie Brilliant Blue G250, 1.6% Orthophosphoric Acid, 8% Ammonium Sulphate, 20% Methanol, all from Sigma-Aldrich). Gels were detained in 1% Acetic acid in distilled water (several changes) until the background was clear. Protein bands were cut-out of the gel and washed twice in 50% Acetonitrile (ACN)/50 nM Ammonium Bicarbonate (AB, Sigma-Aldrich) for 45 minutes at 37°C with agitation. The gel fragments were then incubated at 56°C for 1 hour in 50 mM DTT in 10% ACN/50 mM AB then in 100 mM in 10% ACN/50 mM AB for 30 minutes at room temperature in the dark. Bands were washed twice in 10% ACN/40 mM AB for 15 minutes and dried under vacuum until completely dry. Trypsin (Promega, Southampton UK) was then added on the bands at 200 µg/ml in 10% ACN/40 mM AB and left overnight at 37°C. Supernatant was then collected and bands were washed twice in 3% Formic acid for 1 hour at room temperature under agitation. Supernatants were collected and pooled together after all washes and samples were dried under vacuum, resuspended in 20 µl in 0.1% formic acid in 2% ACN. 10 µl of the purified samples was subjected to an LC-MS/MS analysis using a gradient of 2–36% ACN in 0.1% formic acid over 30 minutes at 350 nL/min using a Dionex Ultimate 3000 HPLC system, as already described in the section: **Identification of PEPITEM.**

### Biacore assay

All Biacore was performed with the help of Dr. Catherine McDonnell (GE Healthcare) using a Biacore™ T200 system (GE Healthcare). To test peptide binding to CDH15, recombinant CDH15-Fc (50 µg/ml) (R&D Systems) was immobilized on protein A bound to a chip using a standard protocol (900s, 5 µl/min). N-terminal biotinylated PEPITEM (24 µg/ml to 770 µg/ml) in HBS-P buffer (GE Healthcare), 5mM CaCl<sub>2</sub> and 0.05% P20 was flowed over the chip at a flow rate of 30 µl/min for 60s injection and 600s dissociation. For this experiment,

Buffer alone and random peptides were used as controls in case of any non-specific binding, as well as scrambled biotinylated PEPITEM. Binding kinetics were measured in response units (RU) and 'BiaEvaluation' software was used to analyze the data traces.

### Quantification of PEPITEM

500,000 negatively selected B cells were incubated in the presence or absence of adiponectin 15 µg/ml for 1 hour at room temperature. After centrifugation at 250 g for 7 minutes, supernatants were 'spiked' with 10 ng <sup>3</sup>H (tritium) radiolabelled PEPITEM as an internal mass standard for relative intensity quantification. Peptides were purified on DSC-18 solid phase extraction columns as described above and analyzed by LC-MS/MS as described above. Due to their identical chromatographic properties, endogenous and synthetic radiolabelled versions of PEPITEM elute at the same point on the gradient, allowing comparison in the same mass spectrum. However, due to their different physical properties, these versions are readily resolved as separate peaks within this mass spectrum. Therefore, extracted ion chromatograms (EIC) comparing intensity of the 10 ng radiolabelled standard (m/z 780.88±0.05) to that of endogenous PEPITEM (m/z 774.88±0.05) allowed quantification of the native peptide. This method of relative intensity quantification is time-honoured within the field of analytical science<sup>62</sup>.

Alternatively, B cell subsets were isolated by automated cell sorting using a Moflow Astrios EQ (Beckman Coulter) and labelled as previously described in the section: *In vitro* transmigration assay. The B cell subsets were then incubated with 15 µg/ml of adiponectin for one hour. Supernatants were collected and analyzed by mass spectrometry to quantify PEPITEM using the radiolabelled quantification method.

Samples for the PEPITEM secretion time-course were collected after 5, 15, 30 minutes, 1, 3 and 24 hours after PEPITEM incubation on endothelial cells. Samples were centrifuged, purified on C18 columns at 100% ACN and analyzed by MS using the radiolabelled quantification method.

### Identifying changes in the affinity of $\alpha_L\beta_2$ on lymphocytes

96 well plates were coated with 50 µg/ml of recombinant ICAM-1/Fc (R&D Systems) overnight at 4°C. The plate was blocked using PBS 2% BSA for an hour at room temperature and PBL treated with CXCL10 (80 ng/ml) and/or S1P (10 µM) were added for 6 minutes. Excess of unbound PBL was washed away. Bound PBL were collected using cold PBS by rough pipetting and PBL were labelled at 4 °C for the lymphocyte integrin  $\alpha_L\beta_2$  (LFA-1) using the mouse anti-human KIM127 (10 µg/ml) antibody recognizing the intermediate affinity epitope (Nancy Hogg, London) or the S1PR1 antibody (5 µg/ml; Cayman chemicals; amino acids 241–253 (ISKASRSSEKSLA)). KIM127 was detected using a goat anti-mouse Alexa 488 secondary antibody (Invitrogen) at 8 µg/ml and S1PR1 with a donkey anti-rabbit Alexa 488 secondary antibody (Invitrogen) at 8 µg/ml. The expression of the affinity site was measured on memory T cells (CD45RO<sup>+</sup> CD3<sup>+</sup> T cells) by flow cytometry as described in the section: **Flow cytometry**. To measure the expression of S1PRs on firmly adhered and transmigrated memory T cells, we washed the endothelial cells after 6 minutes of PBL transmigration using cold EDTA (Sigma-Aldrich). The EDTA

wash was repeated until all firmly adhered cells were recovered. Transmigrated cells were collected with endothelial cells using accutase for one minute at 37°C and firmly adhered and transmigrated cells were labelled with CD45RO-APC (1:20) (UCHL1) (BD Bioscience) and CD3-PerCp-Cy5.5 (1:50) (OKT3) (Ebioscience) and S1PR1 and analyzed by flow cytometry.

### Investigating the function of PEPITEM in mouse models of inflammation

All experiments were performed in accordance with United Kingdom Home Office regulations. For the animal studies, in each experiment B cell-deficient or wild-type (WT) animals with the same background were allocated at random to different experimental groups. Importantly, mice from the same litter were randomly distributed amongst the experimental groups and where possible, were equally distributed amongst experimental groups. Comparison of peptide, scrambled peptide, and carrier (PBS) were carried out on the same day with identical reagents when possible.

**Acute peritoneal inflammation**—BALB/c WT or BALB/c B cell-deficient mice (*Igh-J<sup>tm1Dhu</sup>* N<sup>+</sup>+N2, these mice carry a deletion of the J segments of the Ig heavy chain locus) (Taconic, New York, USA) were housed in the Biomedical Services Unit at the University of Birmingham. Mice were used between 6 and 8 weeks of age and were matched for sex as both male and females were used. Peritonitis was induced by the intraperitoneal injection (i.p) of 1 mg of type A zymosan (Sigma-Aldrich) as previously described<sup>63</sup>. In some animals zymosan was delivered with 300 µg PEPITEM or scrambled peptide. Cells washed from the peritoneal cavity were collected in PBS at 48 hours post injection. Erythrocytes in the peritoneal exudates were lysed and leukocytes stained for analysis by flow cytometry. Tubes containing the cells from the peritoneal exudates were fully acquired on the flow cytometry to accurately count the cells. Gates were set up on all cells in the peritoneum and the number of T cells was determined based on CD3 expression. Blood was drawn by cardiac puncture under the armpit and processed as for peritoneal exudate cells. All data was normalized to the number of T cells in WT mice treated with zymosan.

**Systemic bacteraemia upon Salmonella infection in the liver**—For Salmonella infections, attenuated *Salmonella* Typhimurium (strain SL3261, originally obtained from Dr RA Kingsley (Wellcome Trust Sanger Institute, Cambridge<sup>64</sup>) was grown overnight and bacteria were harvested from log phase cultures as described previously<sup>65</sup>. C57BL/6 WT or C57BL/6 B cell-deficient (B cell-deficient mice were generated in house from breeding out the QM (quasi-monoclonal) IgH transgene from QM mice, which have the other IgH locus inactivated)<sup>66</sup> mice were infected by intraperitoneal injection with  $5 \times 10^5$  *S. Typhimurium* in PBS containing 100 µg PEPITEM. Mice were used between 6 and 8 weeks of age and were matched for sex as both male and females were used. Control mice received  $5 \times 10^5$  *S. Typhimurium* in PBS only. Mice received further PEPITEM (or PBS) injections (100 µg i.p.) daily for the next 4 days and all samples were collected at day 5 or 7 post-infection. Livers were immediately frozen and were subsequently examined by immunohistochemistry (IHC) as has been described elsewhere<sup>67</sup>. All IHC was performed in Tris buffer (pH 7.6) at room temperature. Primary antibodies specific for CD3 (1:300) (145-2C11, BD Pharmingen) and F4/80 (1:500) (Cl:A3:1, AbD Serotec), and secondary antibodies (Dako



Cytomation) (horse-radish peroxidase- (1:300) or biotin-conjugated (1:600)) were added for 60 and 45 minutes respectively. Slides were developed using 3, 3'-diaminobenzidine tetrahydrochloride (Sigma-Aldrich) or alkaline-phosphatase (ABCComplex, Vector Laboratories) and levamisole with naphthol AS-MX phosphate and Fast Blue BB salt (all from Sigma-Aldrich) respectively. Slides were mounted in glycerol (Sigma-Aldrich) and images acquired using a Leica CTR6000 microscope (Leica, Milton Keynes, UK) with Image J and QCapture software. Mean CD3<sup>+</sup> cells per foci were quantified for a minimum of 50 foci per tissue section at x25 magnification.

**Acute liver ischemia and reperfusion injury**—Splenic T cells were isolated from 8–10 week old male C57BL/6 WT mice (Harlan, Oxford, UK) through negative selection magnetic activated cell sorting (MACS) using the Pan T cell isolation kit II (Miltenyi Biotec, Surrey, UK) according to the manufacturer's instructions. C57BL/6 mice were anaesthetised by intraperitoneal injection of ketamine (100 mg/Kg, Vetlar V, Pfizer, Kent, UK) and xylazine hydrochloride (10 mg/Kg, Xylacare, Animalcare, York, UK) delivered in 0.9% saline solution. The trachea and right common carotid artery were cannulated and the liver was exposed. Prior to ischemia, 250 µl of PEPITEM or scrambled peptide was injected via the carotid artery and allowed to circulate for 5 minutes. Ischemia of the left and median lobes of the liver was induced through application of a traumatic vascular clamp to the hepatic artery and portal vein supplying these lobes for 90 minutes. After 90 minutes of ischemia the clamp was removed and intravital observations carried out. Using an Olympus IX81 inverted microscope (Olympus, UK) the microvasculature of the liver was viewed through a 10X objective. 1 million fluorescently labelled T cells (CFDA-SE, 10 µM, Life Technologies, Paisley, UK) with 20 µl of PEPITEM/scrambled peptide were injected into the carotid artery at the point of clamp removal. A random field was selected every 10 minutes and imaged for 20 seconds. Five additional fields of view in a pre-defined pattern were then imaged for 20 seconds each. Adherent cells were defined as cells that were static for at least 20 seconds. Cells were counted on each field.

**Acute model of LPS (Lipopolysaccharide) driven uveitis (EIU-experimental autoimmune uveitis)**—C57BL/6J WT mice were originally obtained from Harlan UK Limited (Oxford, U.K.), and breeding colonies were established within the Animal Services Unit at Bristol University (Bristol, U.K.). Mice were housed in specific pathogen-free conditions with continuously available water and food. Female mice immunized for disease induction were aged between 6 and 8 weeks. All mice were kept in the animal house facilities of the University of Bristol. Treatment of animals conformed to United Kingdom legislation and to the Association for Research in Vision and Ophthalmology statement for the Use of Animals in Ophthalmic and Vision Research.

**EIU Induction and therapeutic intervention:** Local administration of LPS from *Salmonella* Typhimurium (50ng/eye) (Sigma-Aldrich) was performed by intravitreal injection in anaesthetised B6LY5 mice as previously described<sup>68</sup>. Animals were anaesthetised by i.p injection of 150 µl of Vetalar (ketamine hydrochloride 100mg/ml; Pfizer, Sandwich, UK) and Rompun (xylazine hydrochloride 20mg/ml; Bayer, Newburg, UK) mixed with sterile water in a ratio of 0.6:1:84. The pupils of all animals were dilated using topical

tropicamide 1% (Minims from Chauvin Pharmaceuticals Ltd, UK). Intravitreal injections were performed under the direct control of a surgical microscope with the tip of a 12 mm 33-gauge hypodermic needle mounted on a 5 µl syringe (Hamilton AG, Bonaduz, Switzerland). For treatment groups either PEPITEM (6 µg) or PBS were combined with 50ng/eye of LPS as a single injection, administered in a total volume of 4 µl per injection. The injection site was treated with chloramphenicol ointment.

**Isolation of ocular infiltrate:** At 15 hours following LPS/treatment administration, eyes were enucleated and carefully cleaned to remove all extraneous connective and vascular tissue. The aqueous & vitreous humour, iris, ciliary body and retina were microscopically dissected in HBSS (Life Technologies, Paisley, UK). These ocular components were homogenized and forced through a 70 µm cell strainer with a syringe plunger, to obtain a single-cell suspension, and stained for flow cytometry analysis.

**Flow cytometric analysis of ocular infiltrate:** Cells were incubated with 24G2 cell supernatant for 10 minutes at 4°C before incubation with fluorochrome-conjugated monoclonal antibodies (all from BD Bioscience, Oxford, UK) against cell surface markers CD45 (1:1000) (30-F11), CD4 (1:100) (RM4-5) and CD8 (1:100) (53-6.7) at 4°C for 20 minutes. Cells were resuspended in 7-aminoactinomycin D (7AAD) (Molecular Probes), and dead cells were excluded from analysis by gating on 7AAD negative cells. Measurement of cell suspensions were acquired using a three-laser BD LSR-II flow cytometer (BD Cytometry Systems, Oxford, UK) and analyzed was performed using FlowJo software version 7.6.5 (Tree Star, Ashland, OR). Cell numbers were calculated by reference to a known cell standard, as previously reported<sup>64</sup>. Briefly, splenocytes at a range of known cell concentrations were acquired using a fixed and stable flow rate for 1 minute. Based on total cell number acquired during this time, a standard curve was generated and used to interpolate cell concentrations of ocular infiltrating cells acquired at the same flow rate and time.

### **Virally induced Sjögren's syndrome**

**Mice and salivary gland cannulation:** C57BL/6 mice were from Harlan. Under ketamine-domitor (Pfizer, Sandwich, UK) anesthesia, the submandibular glands of female C57BL/6 mice (8–12 weeks old) were intraductally cannulated with 10<sup>8</sup>–10<sup>9</sup> pfu of luciferase-encoding replication-defective adenovirus (AdV5), as previously described<sup>40</sup>. A group of 5 mice were administered (i.p injections) 100 µg PEPITEM and another group of 5 mice were administered 100 µg scrambled peptide every day until day 5 post-cannulation (p.c.).

**Histology and Immunofluorescence:** Salivary glands from cannulated mice treated with PEPITEM and scrambled peptides were harvested, snap frozen in OCT (Sakura, UK) over liquid nitrogen. Frozen sections of 7 µm in thickness were cut, left to dry overnight at room temperature, next day they were stored in –80°C until use. For immunofluorescence analysis, slides were allowed to come to room temperature and then fixed for 20 minutes in ice-cold acetone, left to dry and then were hydrated in PBS. For immunofluorescence staining, all dilutions of reagents and antibodies were made in PBS with 1% BSA. Firstly, to block endogenous biotin sections were treated with 0.05% avidin (Sigma-Aldrich) and

0.005% biotin (Sigma-Aldrich) for 15 minutes each and a washed for 5 minutes with PBS in between the two incubations. Followed by, blocking with 10% horse serum (Sigma-Aldrich) for 10 minutes. Slides were then incubated for 60 minutes with 'cocktails' containing the following primary antibodies in PBS (1% BSA); CD19 Alexa Fluor647 (1:50) (eBio1D3), CD3 $\epsilon$  biotin (1:50) (ebio500A2) (both were from Ebioscience). Biotinylated CD3 $\epsilon$  was detected using streptavidin-Alexa Fluor 555 (1:500) (Molecular Probes). Hoechst (1:1000) (Molecular Probes) was used for nuclear stain. All secondary antibodies were incubated for 30 minutes. Slides were mounted with Prolong Gold Antifade reagent (Life Technologies).

Images were acquired on a Zeiss 780 upright confocal head with a Zeiss Axio Imager Z1 microscope and viewed through a 10X objective. Digital images were recorded in three separately scanned channels with no overlap in detection of emissions from the respective fluorochromes. Confocal micrographs were stored as digital arrays of 1024 $\times$ 1024 pixels with 8-bit sensitivity; detectors were routinely set so that intensities in each channel spanned the 0–255 scale optimally. The Zen 2010 Software was used to process these images.

**Isolation of leukocytes:** Cannulated salivary glands were harvested and chopped into small pieces and digested for 20 minutes at 37°C with gentle stirring in 2 ml RPMI 1640 medium (Sigma-Aldrich) containing collagenase dispase (250  $\mu$ g/ml; from Roche, Welwyn, UK), DNase I (25  $\mu$ g/ml; from Sigma-Aldrich) and 2% (vol/vol) FCS. The suspension was gently pipetted to break up aggregates. During the final pipetting, EDTA (Sigma-Aldrich) was added to a final concentration of 10 mM to further reduce cell aggregates. Cells were then passed through a 70  $\mu$ m mesh with a syringe, were washed twice and resuspended in PBS (with 0.5% BSA and 2 mM EDTA)

**Flow cytometry:** Single cells suspensions were stained for 30 minutes in PBS (with 0.5% BSA and 2 mM EDTA) with 'cocktails' of the following antibodies CD3 $\epsilon$  PECy7 (1:200) (145-2C11), CD19 APC-Cy7 (1:100) (eBio1D3) (from EBiosciences). Cells were then washed twice in PBS (with 0.5% BSA and 2 mM EDTA), resuspended in PBS (with 0.5% BSA and 2 mM EDTA) and then analyzed using a Cyan-ADP (Dako) with forward/side scatter gates set to exclude non-viable cells. Data were analyzed with FlowJo software (Tree Star, Oregon, USA).

## Patient studies

Sample size for the patient studies were guided by the variance from a previous study in our laboratory in which we determined the frequency of adiponectin receptors on monocytes from individuals with T1D versus matched healthy controls<sup>7</sup>. Randomization was not required for this study. All patients and controls were analyzed in parallel on the same flow cytometer over a period of weeks, as they became available from clinic. The expression of the adiponectin receptors was always determined compared to the isotype control for each sample. The same batch numbers of flow cytometry reagents was used throughout to ensure standardisation and reduce inter-experimental variation.

**T1D**—Individuals with T1D were recruited from University Hospital Birmingham Department of Diabetes outpatient clinics. Individuals had received a diagnosis of T1D

fulfilling the 1999 WHO framework<sup>65</sup>. Blood samples were obtained with written informed consent and approval from the Birmingham, East, North and Solihull Research Ethics Committee (06/Q2703/47).

Healthy volunteers were matched to the T1D cohort on gender, age and BMI (Clinical parameters in Supplementary Table 6 and 7). AdipoR1/2 expression on B cells was measured in 19 healthy controls (58% males) and 29 individuals with T1D (65% male). Quantification of PEPITEM secretion by B cells under adiponectin stimulation was measured in 10 healthy controls (60% males) and 10 individuals with T1D (60% males). Lymphocyte transmigration was measured for 15 healthy controls (55% males) and 9 (for the PEPITEM cohort) or 22 (for the adiponectin cohort) individuals with T1D (60% males).

**Rheumatoid arthritis**—Individuals with rheumatoid arthritis were recruited from the Birmingham Early Arthritis Cohort (BEACON). Rheumatoid arthritis was classified according to 1987 American College of Rheumatology criteria. Blood samples were obtained with written informed consent and approval from the NRES committee West Midlands, the Black Country (2/WM/0258). Healthy volunteers were matched to the rheumatoid arthritis cohort on gender and age (Clinical parameters in Supplementary Table 8). AdipoR1/2 expression on B cells was measured in 10 healthy controls (30% males) and 12 individuals with rheumatoid arthritis (41% males). Lymphocyte transmigration was measured for 7 healthy controls (57% males) and 8 individuals with rheumatoid arthritis (12.5% males).

**Ageing study**—AdipoR1/2 expression on B cells was measured in 40 healthy volunteers ranging in age from 21 to 66 years old.

## Statistics

*In vitro* data are from at least 3 experiments including 3 separate donors for PBL, HUVEC or HDMEC and are the mean of these different experiments  $\pm$  s.e.m or SD as stated. Numbers of animals in each model are stated in the figure legends. The number of individuals with T1D or RA, or healthy controls compared is stated in the figure legends. Differences were analyzed using GraphPad Prism software (GraphPad software Inc., LaJolla, USA) by paired or unpaired t-test or by one way ANOVA followed by post hoc analysis for multiple group comparison (Dunnett or Bonferroni). A Dunnett post hoc analysis was used to compare all the data sets on the graph to a common control. A Bonferroni post hoc test was used to compare all data sets in a graph with each other. Normality was checked using the Kolmogorov-Smirnov test. A non-parametric test (Mann-Whitney test) was used when data did not pass the normality test. The Wilcoxon signed rank test was used to compare a data set to a normalized control, where the data was presented as a percentage of that control (i.e. where control values were the same, e.g 100%). P values 0.05 were considered significant.

## Supplementary Material

Refer to Web version on PubMed Central for supplementary material.

## ACKNOWLEDGMENTS

The authors thank Anette Sams and Soren Tullin from Nova Nordisk for providing high molecular weight recombinant adiponectin. We are grateful to Neil Shimwell and Douglas Ward for assistance with mass spectrometry, and Gemma Pui Choy for her help with animal experiments (all from the University of Birmingham, UK). Thanks also to Nancy Hogg (Cancer research UK, London Research Institute, UK) for the activation epitope sensitive anti-LFA-1 antibody, KIM127. We also thank Debbie Hardie for helping with the automated cell sorting (University of Birmingham, UK) and the University of Bristol Flow Cytometry Facility. We thank Peter Nightingale (University Hospitals Birmingham NHS Trust) for advice on statistical analysis.

This work was supported by grants from Diabetes UK (PN, GER) (097825/Z/11/A), the Wellcome Trust (PN, GER) (ISSF 12/13-097825/Z/11/A), an Early Career Award from the Society for Endocrinology (MC), the Medical Research Council (CIC 12011) and a senior fellowship for LSKW (G0802382) and the Juvenile Diabetes Research Foundation (PN, GER) (5-2013-207). Work in the laboratories of GER is supported by the British Heart Foundation at Project Grant (PG/11/49/28983) and Programme Grant (RG/12/7/29693) level. HMM was supported by an Arthritis Research UK Career Development Fellowship (19899). FB is supported by a Wellcome Trust Clinician Scientist Fellowship. AF was supported by an Arthritis Research UK Clinician Scientist Fellowship (18547). The research leading to the RA subject data was funded within the FP7 HEALTH programme under the grant agreement FP7-HEALTH-F2-2012-305549. This report is independent research which was partly supported by the National Institute for Health Research/Wellcome Trust Clinical Research Facility at University Hospitals Birmingham NHS Foundation Trust. The views expressed in this publication are those of the author(s) and not necessarily those of the NHS, the National Institute for Health Research or the Department of Health.

The authors MC, HMM, PN and GER hold patents for the therapeutic and diagnostic use of PEPITEM (WO2013/104928) and cadherin-15 (WO2015/001356) in autoimmune disease, chronic inflammatory disease and other diseases in which T cells contribute to pathogenesis and the use of AdipoRs expression as a biomarker for rheumatoid arthritis (WO2014/080204).

## REFERENCES

1. Cyster JG. Lymphoid organ development and cell migration. *Immunol Rev.* 2003; 195:5–14. [PubMed: 12969306]
2. Koulmanda M, et al. Modification of adverse inflammation is required to cure new-onset type 1 diabetic hosts. *Proc Natl Acad Sci U S A.* 2007; 104:13074–13079. [PubMed: 17670937]
3. Pober JS, Cotran RS. The role of endothelial cells in inflammation. *Transplantation.* 1990; 50:537–544. [PubMed: 2219269]
4. Kadowaki T, et al. Adiponectin and adiponectin receptors in insulin resistance, diabetes, and the metabolic syndrome. *J Clin Invest.* 2006; 116:1784–1792. [PubMed: 16823476]
5. Ouedraogo R, et al. Adiponectin deficiency increases leukocyte-endothelium interactions via upregulation of endothelial cell adhesion molecules in vivo. *J Clin Invest.* 2007; 117:1718–1726. [PubMed: 17549259]
6. Pang TT, et al. Inhibition of islet immunoreactivity by adiponectin is attenuated in human type 1 diabetes. *J Clin Endocrinol Metab.* 2013; 98:E418–428. [PubMed: 23386639]
7. Pang TT, Narendran P. The distribution of adiponectin receptors on human peripheral blood mononuclear cells. *Ann N Y Acad Sci.* 2008; 1150:143–145. [PubMed: 19120283]
8. Lalor PF, Shields P, Grant A, Adams DH. Recruitment of lymphocytes to the human liver. *Immunol Cell Biol.* 2002; 80:52–64. [PubMed: 11869363]
9. Olsson R, Carlsson PO. The pancreatic islet endothelial cell: emerging roles in islet function and disease. *Int J Biochem Cell Biol.* 2006; 38:710–714. [PubMed: 16607697]
10. Andrew DP, et al. Transendothelial migration and trafficking of leukocytes in LFA-1-deficient mice. *Eur J Immunol.* 1998; 28:1959–1969. [PubMed: 9645378]
11. Brezinschek RI, Lipsky PE, Galea P, Vita R, Oppenheimer-Marks N. Phenotypic characterization of CD4+ T cells that exhibit a transendothelial migratory capacity. *J Immunol.* 1995; 154:3062–3077. [PubMed: 7534786]
12. Cinamon G, Shinder V, Alon R. Shear forces promote lymphocyte migration across vascular endothelium bearing apical chemokines. *Nat Immunol.* 2001; 2:515–522. [PubMed: 11376338]
13. Ley K, Laudanna C, Cybulsky MI, Nourshargh S. Getting to the site of inflammation: the leukocyte adhesion cascade updated. *Nat Rev Immunol.* 2007; 7:678–689. [PubMed: 17717539]

14. Ma L, et al. CD31 exhibits multiple roles in regulating T lymphocyte trafficking in vivo. *J Immunol.* 2012; 189:4104–4111. [PubMed: 22966083]
15. Shulman Z, et al. Lymphocyte crawling and transendothelial migration require chemokine triggering of high-affinity LFA-1 integrin. *Immunity.* 2009; 30:384–396. [PubMed: 19268609]
16. Springer TA. Traffic signals on endothelium for lymphocyte recirculation and leukocyte emigration. *Annual review of physiology.* 1995; 57:827–872.
17. McGettrick HM, et al. Direct observations of the kinetics of migrating T cells suggest active retention by endothelial cells with continual bidirectional migration. *J Leukoc Biol.* 2009; 85:98–107. [PubMed: 18948550]
18. Piali L, et al. The chemokine receptor CXCR3 mediates rapid and shear-resistant adhesion-induction of effector T lymphocytes by the chemokines IP10 and Mig. *Eur J Immunol.* 1998; 28:961–972. [PubMed: 9541591]
19. Spiegel S, Milstien S. The outs and the ins of sphingosine-1-phosphate in immunity. *Nat Rev Immunol.* 2011; 11:403–415. [PubMed: 21546914]
20. Jones DA, McIntire LV, Smith CW, Picker LJ. A two-step adhesion cascade for T cell/endothelial cell interactions under flow conditions. *J Clin Invest.* 1994; 94:2443–2450. [PubMed: 7527432]
21. Luscinskas FW, Ding H, Lichtman AH. P-selectin and vascular cell adhesion molecule 1 mediate rolling and arrest, respectively, of CD4+ T lymphocytes on tumor necrosis factor alpha-activated vascular endothelium under flow. *J Exp Med.* 1995; 181:1179–1186. [PubMed: 7532680]
22. Yago T, et al. Analysis of an initial step of T cell adhesion to endothelial monolayers under flow conditions. *J Immunol.* 1995; 154:1216–1222. [PubMed: 7529795]
23. Ahmed SR, et al. Prostaglandin D2 regulates CD4+ memory T cell trafficking across blood vascular endothelium and primes these cells for clearance across lymphatic endothelium. *J Immunol.* 2011; 187:1432–1439. [PubMed: 21715691]
24. Fukuhara S, et al. The sphingosine-1-phosphate transporter Spns2 expressed on endothelial cells regulates lymphocyte trafficking in mice. *J Clin Invest.* 2012; 122:1416–1426. [PubMed: 22406534]
25. Hisano Y, Kobayashi N, Yamaguchi A, Nishi T. Mouse SPNS2 functions as a sphingosine-1-phosphate transporter in vascular endothelial cells. *PLoS One.* 2012; 7:e38941. [PubMed: 22723910]
26. Nijnik A, et al. The role of sphingosine-1-phosphate transporter Spns2 in immune system function. *J Immunol.* 2012; 189:102–111. [PubMed: 22664872]
27. Ledgerwood LG, et al. The sphingosine 1-phosphate receptor 1 causes tissue retention by inhibiting the entry of peripheral tissue T lymphocytes into afferent lymphatics. *Nat Immunol.* 2008; 9:42–53. [PubMed: 18037890]
28. Mandala S, et al. Alteration of lymphocyte trafficking by sphingosine-1-phosphate receptor agonists. *Science.* 2002; 296:346–349. [PubMed: 11923495]
29. Matloubian M, et al. Lymphocyte egress from thymus and peripheral lymphoid organs is dependent on S1P receptor 1. *Nature.* 2004; 427:355–360. [PubMed: 14737169]
30. Pappu R, et al. Promotion of lymphocyte egress into blood and lymph by distinct sources of sphingosine-1-phosphate. *Science.* 2007; 316:295–298. [PubMed: 17363629]
31. Pham TH, Okada T, Matloubian M, Lo CG, Cyster JG. S1P1 receptor signaling overrides retention mediated by G alpha i-coupled receptors to promote T cell egress. *Immunity.* 2008; 28:122–133. [PubMed: 18164221]
32. Hammad SM, Al Gadban MA, Semler AJ, Klein RL. Sphingosine 1-Phosphate Distribution in Human Plasma: Associations with Lipid Profiles. *Journal of Lipids.* 2012; 2012
33. Murata N, K. et al. Interaction of sphingosine 1-phosphate with plasma components, including lipoproteins, regulates the lipid receptor-mediated actions. *Biochem J.* 2000; 352:809–815. [PubMed: 11104690]
34. Sattler K, Levkau B. Sphingosine-1-phosphate as a mediator of high-density lipoprotein effects in cardiovascular protection. *Cardiovascular Research.* 2009; 82:201–211. [PubMed: 19233866]
35. Chen J, et al. Immunoglobulin gene rearrangement in B cell deficient mice generated by targeted deletion of the JH locus. *Int Immunol.* 1993; 5:647–656. [PubMed: 8347558]

36. Johansson C, et al. Elevated neutrophil, macrophage and dendritic cell numbers characterize immune cell populations in mice chronically infected with Salmonella. *Microb Pathog.* 2006; 41:49–58. [PubMed: 16782300]
37. Lalor PF, Lai WK, Curbishley SM, Shetty S, Adams DH. Human hepatic sinusoidal endothelial cells can be distinguished by expression of phenotypic markers related to their specialised functions in vivo. *World J Gastroenterol.* 2006; 12:5429–39. [PubMed: 17006978]
38. Wong J, et al. A minimal role for selectins in the recruitment of leukocytes into the inflamed liver microvasculature. *J Clin Invest.* 1997; 99:2782–90. [PubMed: 9169509]
39. Bombardieri M, et al. Inducible tertiary lymphoid structures, autoimmunity, and exocrine dysfunction in a novel model of salivary gland inflammation in C57BL/6 mice. *J Immunol.* 2012; 189:3767–76. [PubMed: 22942425]
40. Bridges D, Moorhead GB. 14-3-3 proteins: a number of functions for a numbered protein. *Science's STKE : signal transduction knowledge environment.* 2005; 2005:re10. [PubMed: 16091624]
41. Dougherty MK, Morrison DK. Unlocking the code of 14-3-3. *Journal of cell science.* 2004; 117:1875–1884. [PubMed: 15090593]
42. Fu H, Subramanian RR, Masters SC. 14-3-3 proteins: structure, function, and regulation. *Annual review of pharmacology and toxicology.* 2000; 40:617–647.
43. Layfield R, et al. Neurofibrillary tangles of Alzheimer's disease brains contain 14-3-3 proteins. *Neuroscience letters.* 1996; 209:57–60. [PubMed: 8734909]
44. Lodygin D, Hermeking H. The role of epigenetic inactivation of 14-3-3sigma in human cancer. *Cell research.* 2005; 15:237–246. [PubMed: 15857578]
45. Garcia-Guzman M, Dolfi F, Russello M, Vuori K. Cell adhesion regulates the interaction between the docking protein p130(Cas) and the 14-3-3 proteins. *J Biol Chem.* 1999; 274:5762–5768. [PubMed: 10026197]
46. Han DC, Rodriguez LG, Guan JL. Identification of a novel interaction between integrin beta1 and 14-3-3beta. *Oncogene.* 2001; 20:346–357. [PubMed: 11313964]
47. Mhawech P. 14-3-3 proteins--an update. *Cell research.* 2005; 15:228–236. [PubMed: 15857577]
48. Rodriguez LG, Guan JL. 14-3-3 regulation of cell spreading and migration requires a functional amphipathic groove. *J Cell Physiol.* 2005; 202:285–294. [PubMed: 15389601]
49. Choi EY, et al. Regulation of LFA-1-dependent inflammatory cell recruitment by Cbl-b and 14-3-3 proteins. *Blood.* 2008; 111:3607–3614. [PubMed: 18239087]
50. Fagerholm SC, Hilden TJ, Nurmi SM, Gahmberg CG. Specific integrin alpha and beta chain phosphorylations regulate LFA-1 activation through affinity-dependent and -independent mechanisms. *J Cell Biol.* 2005; 171:705–715. [PubMed: 16301335]
51. Yuan Y, et al. Identification of a novel 14-3-3zeta binding site within the cytoplasmic domain of platelet glycoprotein Ibalpha that plays a key role in regulating the von Willebrand factor binding function of glycoprotein Ib-IX. *Circ Res.* 2003; 105:1177–1185. [PubMed: 19875727]
52. Roviezzo F, et al. Sphingosine-1-phosphate modulates vascular permeability and cell recruitment in acute inflammation in vivo. *The Journal of pharmacology and experimental therapeutics.* 2011; 337:830–837. [PubMed: 21421740]
53. Metha D, Konstantoulaki M, Ahmed GU, Malik AB. Sphingosine 1-Phosphate-induced Mobilization of Intracellular Ca<sup>2+</sup> Mediates Rac Activation and Adherens Junction Assembly in Endothelial Cells. *The Journal of Biol Chem.* 2005; 280:17320–17328. [PubMed: 15728185]
54. LeBien TW, Tedder TF. B lymphocytes: how they develop and function. *Blood.* 2008; 112:1570–1580. [PubMed: 18725575]
55. Serreze DV. B lymphocytes are essential for the initiation of T cell-mediated autoimmune diabetes: analysis of a new "speed congenic" stock of NOD.Ig mu null mice. *J Exp Med.* 1996; 184:2049–2053. [PubMed: 8920894]
56. Finnegan A, Ashaye S, Hamel KM. B effector cells in rheumatoid arthritis and experimental arthritis. *Autoimmunity.* 2012; 45:353–363. [PubMed: 22432771]
57. Pescovitz MD. Rituximab, B-Lymphocyte Depletion, and Preservation of Beta-Cell Function. *N Engl J Med.* 2009; 361:2143–52. [PubMed: 19940299]

58. De Vita S, et al. Efficacy of selective B cell blockade in the treatment of rheumatoid arthritis. Evidence of a pathogenic role for B cells. *Arthritis and rheumatism*. 2002; 46:2029–2033. [PubMed: 12209504]

## METHODS-ONLY REFERENCES

59. Rainger GE, Stone P, Morland CM, Nash GB. A novel system for investigating the ability of smooth muscle cells and fibroblasts to regulate adhesion of flowing leukocytes to endothelial cells. *J Immunol Methods*. 2001; 255:73–82. [PubMed: 11470288]
60. Cooke BM, Usami S, Perry I, Nash GB. A simplified method for culture of endothelial cells and analysis of adhesion of blood cells under conditions of flow. *Microvasc Res*. 1993; 45:33–45. [PubMed: 8479340]
61. Butler LM, Rainger GE, Rahman M, Nash GB. Prolonged culture of endothelial cells and deposition of basement membrane modify the recruitment of neutrophils. *Exp Cell Res*. 2005; 310:22–32. [PubMed: 16109405]
62. Eidhammer, I., et al. *Computational and Statistical Methods for Protein Quantification by Mass Spectrometry*. John Wiley & Sons; New Jersey: 2012.
63. Rajakariar R, et al. Novel biphasic role for lymphocytes revealed during resolving inflammation. *Blood*. 2008; 111:4184–4192. [PubMed: 18218853]
64. Hoiseth SK, Stocker BA. Aromatic-dependent *Salmonella typhimurium* are non-virulent and effective as live vaccines. *Nature*. 1981; 291:238–9. [PubMed: 7015147]
65. Cunningham AF, et al. Responses to the soluble flagellar protein FliC are Th2, while those to FliC on *Salmonella* are Th1. *Eur J Immunol*. 2004; 34:2986–95. [PubMed: 15384042]
66. Cascalho M, A. et al. A quasi-monoclonal mouse. *Science*. 1996; 272:1649–1652. [PubMed: 8658139]
67. Flores-Langarica A, et al. Systemic flagellin immunization stimulates mucosal CD103+ dendritic cells and drives Foxp3+ regulatory T cell and IgA responses in the mesenteric lymph node. *J Immunol*. 2012; 189:5745–54. [PubMed: 23152564]
68. Kerr EC, et al. Analysis of retinal cellular infiltrate in experimental autoimmune Uveoretinitis reveals multiple regulatory cell populations. *J. Autoimmun*. 2008; 31:354–361. [PubMed: 18838247]
69. Alberti KG, Zimmet PZ. Definition, diagnosis and classification of diabetes mellitus and its complications. Part 1: diagnosis and classification of diabetes mellitus provisional report of a WHO consultation. *Diabetic medicine : a journal of the British Diabetic Association*. 1998; 15:539–53. [PubMed: 9686693]



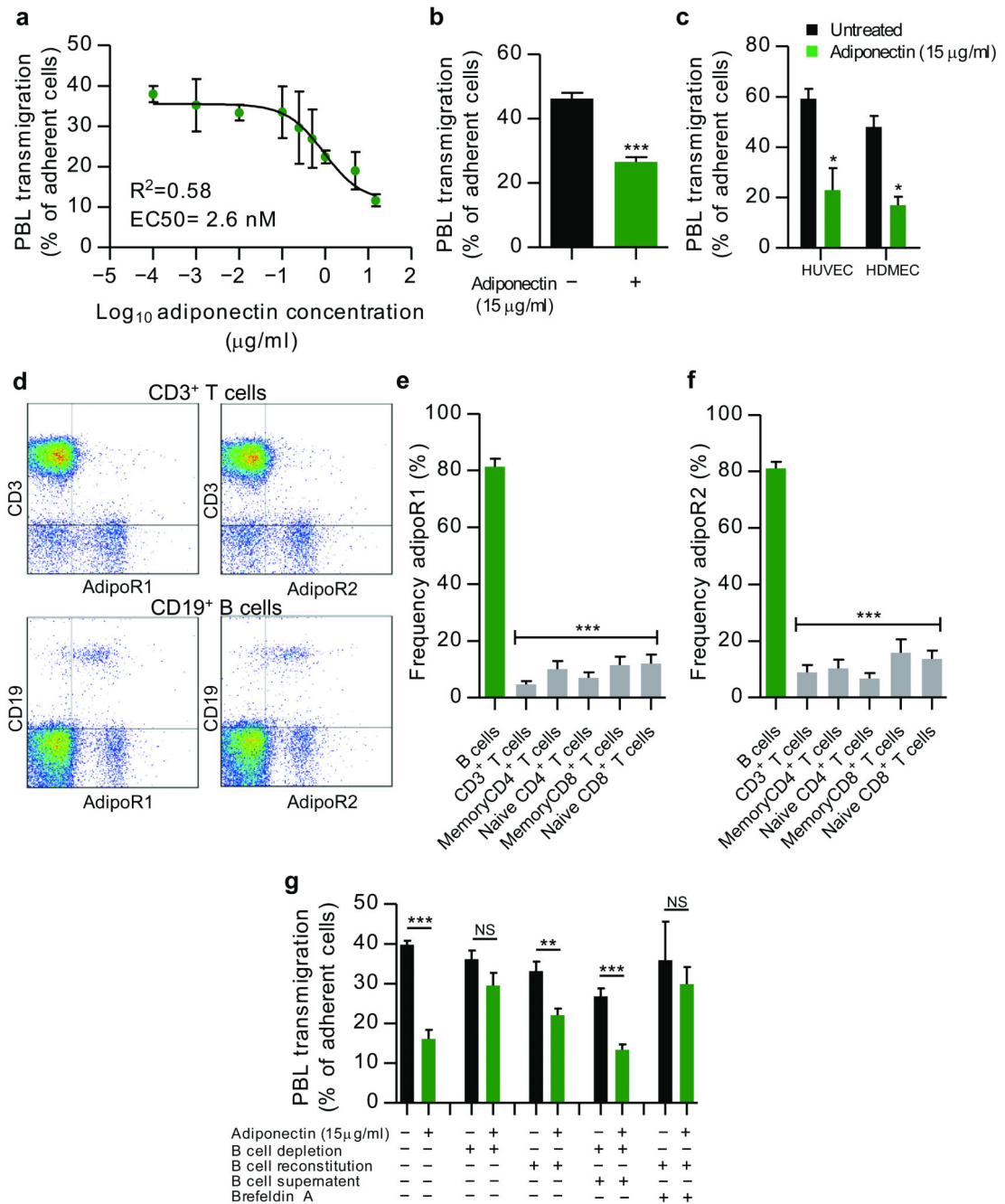


**Figure 1. T cell migration across endothelial cells is regulated by a soluble agent released from B cells stimulated with adiponectin**

(a-c) The effects of adiponectin (0–15 μg/ml) on T cell migration across TNF-α&IFN-γ treated (a) HUVECs under static (n=3–7) or (b) flow conditions (n=6), or (c), HDMEC under static conditions (n=3–4). (d) Representative plots of Adiponectin receptor-1 and -2 (AdipoR1 and 2) expression on T cells (CD3<sup>+</sup>) and B cells (CD19<sup>+</sup>) measured by flow-cytometry. (e, f) Percentage of adiponectin receptor positive cells on lymphocyte subpopulations (measured by flow-cytometry), n=6–13. (g) Transmigration of T cells

following B cell depletion, reconstitution of depleted preparations with B cells or B cell supernatant or inhibition B cell secretion by Brefeldin A (10  $\mu\text{g/ml}$ ),  $n=3-7$ . Data are from at least 3 independent experiments using 3 donors for both PBL and HUVEC/HDMEC and are  $\text{mean}\pm\text{s.e.m.}$  NS: not significant, \*  $P$  0.05, \*\*  $P$  0.01, \*\*\*  $P$  0.001 by (a) linear regression (b-c, g) paired t-test compared to untreated (no adiponectin) control or (e, f) Dunnett post-test compared to B cells.

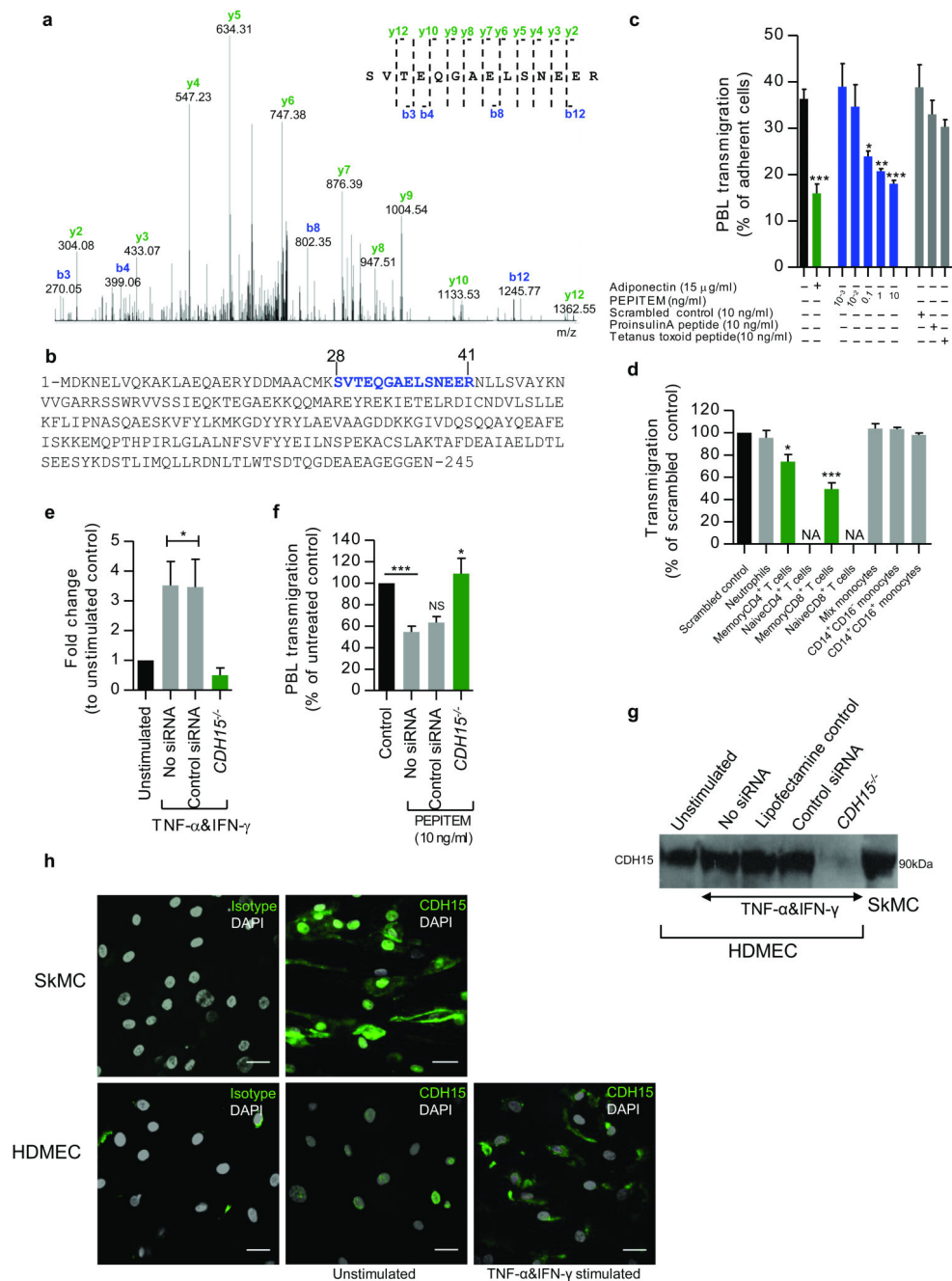


**Figure 2. PEPITEM inhibits T cell transmigration by binding to Cadherin-15 on endothelial cells**

(a) MS/MS analysis of ion m/z 774.8 with the predicted sequence for PEPITEM, data representative of n=3. (b) Amino acid sequence of 14.3.3.ζδ with PEPITEM highlighted in blue. (c) The effect of PEPITEM (0–10 ng/ml), scrambled control peptide or irrelevant peptides (proinsulin chain A and Tetanus toxoid peptide at 10 ng/ml) on PBL transmigration, n=3–4. (d) The effect of PEPITEM on the transmigration of pre-sorted leukocyte populations. Data normalized to scrambled control peptide, n=3–6. NA= no

adhesion. **(e, f)** The effects of control or *cadherin-15* (*CDH15*) specific siRNA on **(e)** the mRNA expression of *CDH15* in HDMECs (n=6) and **(f)** on T cell transmigration across HDMECs (n=6). Data normalized to **(e)** unstimulated or **(f)** untreated and no siRNA control. **(g-h)** The effects of control or *CDH15* specific siRNA on the protein expression of CDH15 determined by **(g)** Western Blot or **(h)** confocal microscopy in HDMEC and skeletal muscle cells (SkMC). Scale bars: 30  $\mu$ m. Data are mean $\pm$ s.e.m. \* *P* 0.05, \*\* *P* 0.01, \*\*\* *P* 0.001 compared to **(c)** no adiponectin/PEPITEM control, **(d)** scrambled control and **(e, f)** unstimulated control or no siRNA by Dunnett post-test.

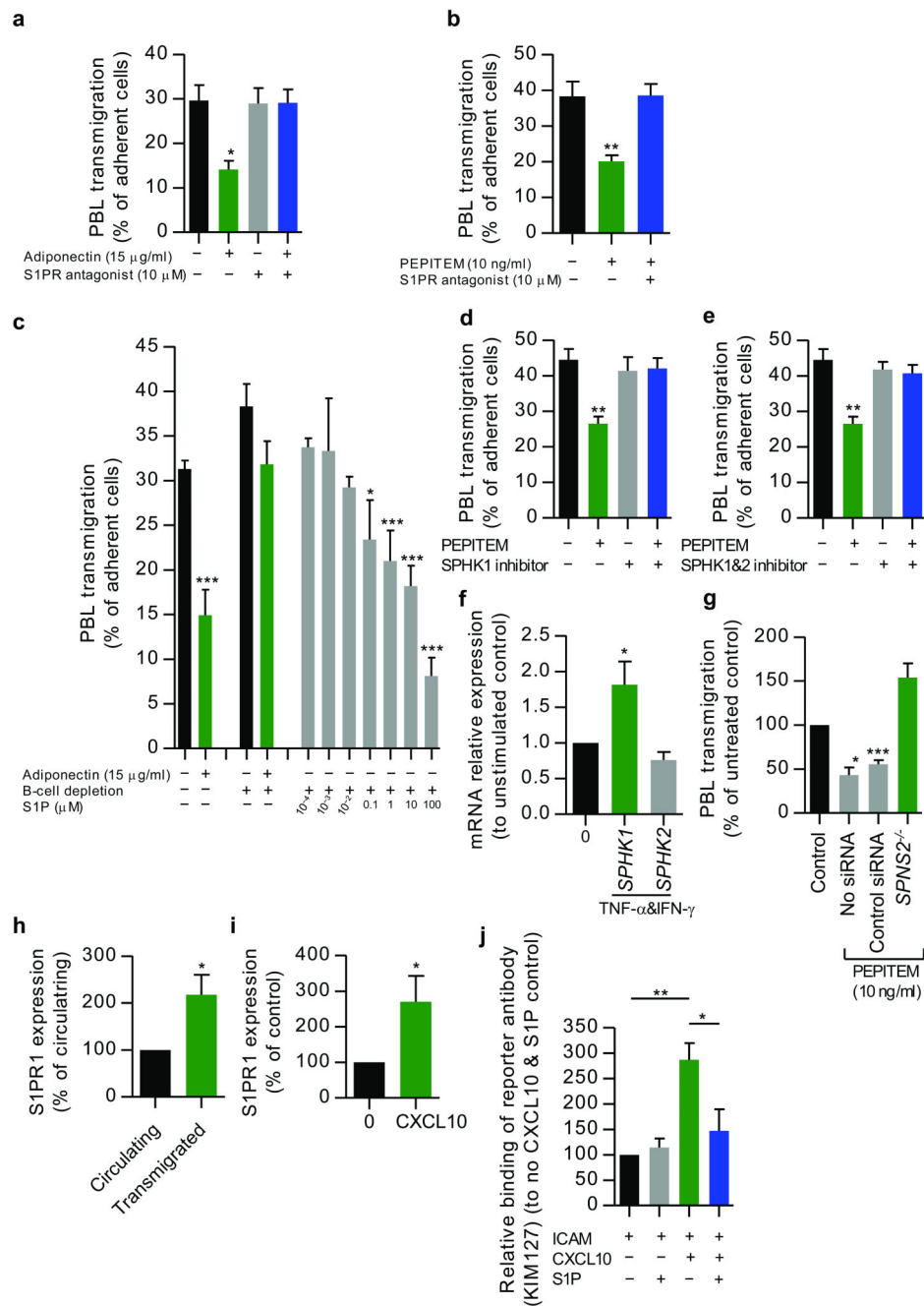


**Figure 3. PEPITEM induces the S1P release from endothelial cells which inhibits T cell migration**

(a, b) The effects of an S1PR antagonist (10  $\mu$ M) on T cell migration in the presence or absence of (a) adiponectin (n=3–5) or (b) PEPITEM (n=3–7). (c) The effects on T cell transmigration of adding S1P to B cell depleted PBL n=3–6. (d, e) The effects of (d) SPHK1 specific inhibitor (5  $\mu$ M) or (e) SPHK1/2 inhibitor (5  $\mu$ M) on T cell transmigration in the presence of PEPITEM, n=3. (f) The expression of *SPHK1* and *SPHK2* mRNA in endothelial cells, n=7–8. (g) The effect of *SPNS2* specific siRNA on T cell transmigration in the

presence of PEPITEM, n=4. **(h, i)** The expression of S1PR1 on memory T cells (CD3<sup>+</sup>CD45RO<sup>+</sup>) on **(h)** stimulated endothelial cells (n=3) and **(i)** on plated ICAM-1 stimulated with CXCL10 (n=6). **(j)** The effects of S1P on the expression of the LFA-1 activation epitope (KIM127) on ICAM-1 adherent memory T cells (CD3<sup>+</sup>CD45RO<sup>+</sup>) stimulated with CXCL10, n=4. Data are mean±s.e.m and **(g-j)** normalized to control. \* *P* 0.05, \*\* *P* 0.01, \*\*\* *P* 0.001 compared to untreated control by ANOVA and **(a-g)** Dunnett compared to **(a-b, d-e, g)** untreated control or **(c)** B cell depletion no adiponectin control or to **(f)** unstimulated (0) control or **(j)** Bonferroni post-test or **(h)** paired t-test on raw data or **(i)** Wilcoxon signed rank test.

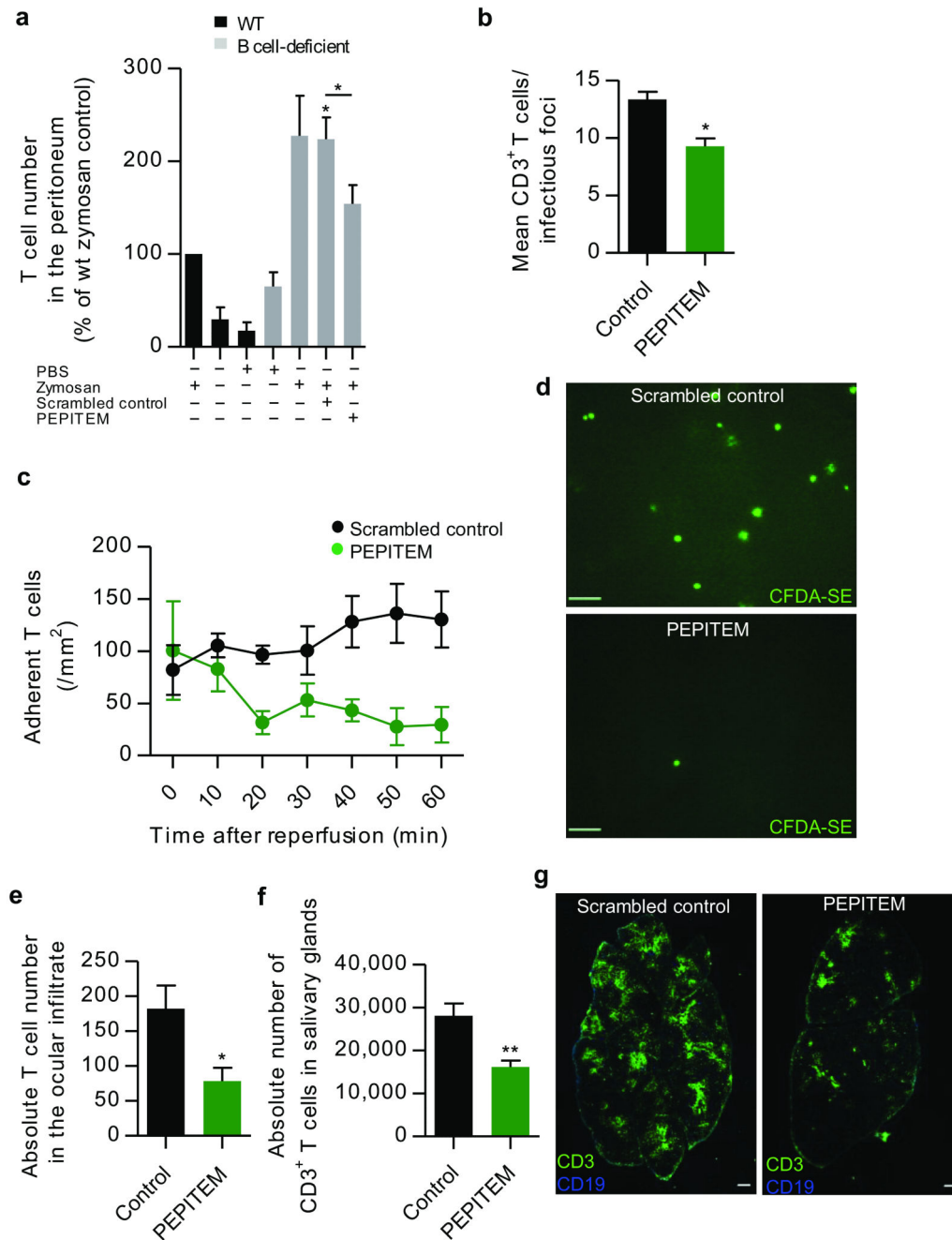


**Figure 4. PEPITEM inhibits T cell migration *in vivo***

(a) T cells recruited into the peritoneum of BALB/c B cell-deficient mice after induction of peritonitis using zymosan and treatment with PEPITEM or scrambled peptide. All data was normalized to the number of T cells in BALB/c WT mice treated with zymosan, n=3–8. (b) Mean CD3<sup>+</sup> T cells per infectious foci in the liver of salmonella-infected C57BL/6 B cell-deficient mice treated with PEPITEM or PBS (control), n = 4. (c) Adherent CD3<sup>+</sup> T cells per mm<sup>2</sup> in the liver sinusoid following reperfusion in C57BL/6 WT mice treated with PEPITEM or scrambled peptide by intravital microscopy. (d) Representative pictures of

CFDA-SE labelled T cells in the sinusoids in scrambled (top) and PEPITEM-treated mice (bottom), n=4 per group. Scale bars, 100  $\mu$ m. **(e)** CD3<sup>+</sup> T cells in the ocular infiltrate of C57BL/6 WT mice treated with PBS (control) or PEPITEM after induction of uveitis by intravitreal injection of LPS, n=9–10. **(f)** CD3<sup>+</sup> T cells in the salivary glands of C57BL/6 WT mice treated with scrambled peptide (control) or PEPITEM after induction of Sjögren's syndrome by cannulation of salivary glands and injection of AdV5, n=7–8. **(g)** Representative pictures showing CD3<sup>+</sup> T cells and CD19<sup>+</sup> B cells in the salivary glands after scrambled peptide (left) or PEPITEM (right) treatment. Scale bars, 100  $\mu$ m. Data are mean  $\pm$ s.e.m. \* *P* 0.05, \*\* *P* 0.01 compared to **(a)** zymosan treated WT by Dunnett post-test or compared to **(a, f)** scrambled or **(b, e)** PBS-treated B cell-deficient mice by unpaired t-test, or **(c)** two-way ANOVA.



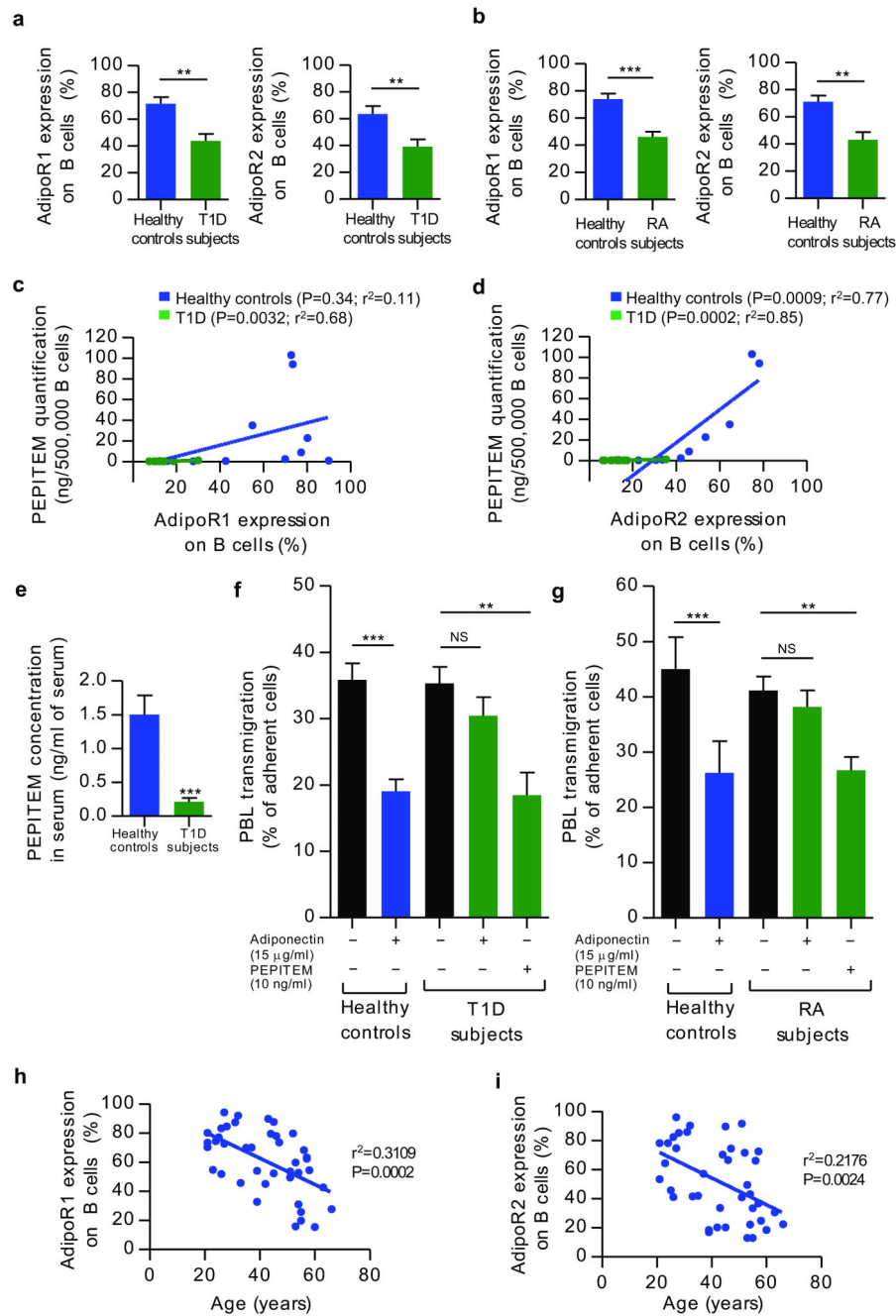


**Figure 5. The PEPITEM pathway is compromised in T1D and rheumatoid arthritis**  
**(a, b)** The expression of (left) adiponectin receptor-1 or (right) adiponectin receptor-2 on B cells in cohorts of healthy controls (**a**: n=19; **b**: n=10) and in **(a)** individuals with T1D (n=29) **(b)** or rheumatoid arthritis (RA) (n=11–12). **(c, d)** Correlation between expression of **(c)** AdipoR1 and **(d)** AdipoR2 on B cells and the quantity of PEPITEM released by B cells following adiponectin stimulation measured by mass spectrometry in healthy controls and individuals with T1D, n=10 in each group. **(e)** Concentrations of PEPITEM in serum from healthy controls and individuals with T1D, n=7. **(f, g)** T cell transmigration in individuals **(f)**

with T1D (n=9–22) or (g) rheumatoid arthritis (RA) (n=7–8) after treatment with adiponectin (15 µg/ml) or PEPITEM (10 ng/ml) or scrambled peptide (10 ng/ml). (h, i) Correlation between expression of (h) AdipoR1 and (i) AdipoR2 on B cells and age in healthy controls, n=40–41. NS= not significant. Data are mean±s.e.m. \*  $P < 0.05$ , \*\*  $P < 0.01$ , \*\*\*  $P < 0.001$  compared to (a) healthy control by Mann-Whitney test or (b, e) unpaired t-test or (f, g) paired t-test for healthy controls and (f, g) ANOVA and Dunnett post-test for individuals with T1D and rheumatoid arthritis (c, d, h, i) by linear regression.

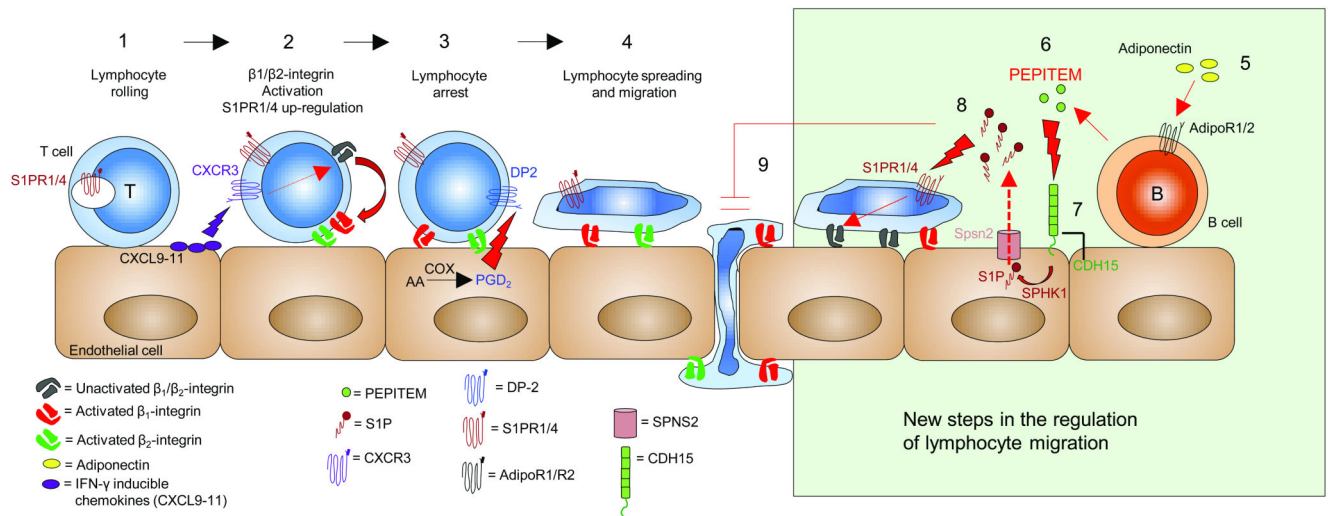


**Figure 6. Schematic depicting B cell-mediated regulation of T cell trafficking during inflammation**

(1) Endothelial cells stimulated with pro-inflammatory cytokines such as TNF- $\alpha$  and IFN- $\gamma$  recruit flowing T cells in the blood. (2)  $\beta_1$ - and  $\beta_2$ -integrins are activated by chemokine signals from CXCL9–11 presented on the endothelial surface which interact with CXCR3 on T cells leading to T cell arrest. At the same time, chemokine stimulation induces S1PR1/4 surface expression on T cells (3). T cell spreading and migration is supported by PGD<sub>2</sub>, generated through the metabolism of arachidonic acid (AA) by cyclooxygenases (COX), which operates through the PGD<sub>2</sub> receptor, DP-2 (4) T cells spread and migrate across and through vascular endothelial cells. (5) Simultaneously, adherent B cells are stimulated by circulating adiponectin through the AdipoR1/2 receptors, (6) resulting in the release of PEPITEM from B cells. (7) PEPITEM binds to Cadherin-15 (CDH15) on endothelial cells, stimulating the release of S1P from endothelial cells. (8) S1P binds to S1P receptors (S1PR1/4) on recruited T cells, (9), which regulates the activation of the  $\beta_2$ -integrin LFA-1 and inhibits trans-endothelial T cell migration.